IEEE Access
Multidisciplinary | Rapid Review | Open Access Journal

Received March 16, 2020, accepted April 4, 2020, date of publication April 22, 2020, date of current version May 7, 2020.

Digital Object Identifier 10.1109/ACCESS.2020.2989516

A Comprehensive Review of Metasurface Structures Suitable for RF Energy Harvesting

ABDULRAHMAN AHMED GHALEB AMER[1], SYARFA ZAHIRAH SAPUAN[1], (Member, IEEE), NASIMUDDIN NASIMUDDIN[2], (Senior Member, IEEE), AROKIASWAMI ALPHONES[3], (Senior Member, IEEE), AND NABIAH BINTI ZINAL[4]

[1]Faculty of Electrical and Electronic Engineering, Universiti Tun Hussein Onn Malaysia, Batu Pahat 86400, Malaysia
[2]Institute for Infocomm Research, A-STAR, Singapore 138623
[3]School of Electrical and Electronic Engineering, Nanyang Technological University, Singapore 639798
[4]Centre for Diploma Studies, Universiti Tun Hussein Onn Malaysia, Batu Pahat 86400, Malaysia

Corresponding authors: Abdulrahman Ahmed Ghaleb Amer (aag2014ye@gmail.com) and Syarfa Zahirah Sapuan (syarfa@uthm.edu.my)

This research was funded by Universiti Tun Hussein Onn Malaysia (UTHM) under TIER 1 research grant, H150.

ABSTRACT Energy harvesting (EH) or scavenging is recognized as harvesting energy from ambient energy sources in the surrounding environment. This paper reports a literature review on radio frequency (RF) EH using different metasurface/metamaterial structures based on split-ring resonators (SRRs), electric inductive–capacitive (ELC) resonators, square-patch unit cells, square-ring unit cells, etc. The essential parameters in rectifying antenna (rectenna) design are included, such as receiving antenna efficiency, conversion efficiency, dimensions, supporting substrate properties, frequency band, and overall performance, etc. It is noted that rectenna design using conventional antennas such as microstrip antennas, monopole antennas, slot antennas, dielectric resonator antennas, etc. suffers from low power conversion efficiency with larger size. To overcome the above-mentioned constraints and enhance the conversion efficiency with smaller size, metasurface/metamaterial structures are used as EH collectors. An introduction to EH is discussed, followed by an overview of energy sources in the ambient environment. Several hypothetical and experimental studies on metasurface-based EH systems are summarized.

INDEX TERMS Metasurface, metamaterial, split-ring resonator, conversion power efficiency, RF energy harvesting, rectenna.

I. INTRODUCTION

As of late, developments on ultra- low power portable electronic devices and wireless sensor networks (WSNs) open the possibility of harvesting ambient energies to power directly low-power electronic devices or recharge secondary batteries. Conversion power efficiency is the important figure of merit of an energy harvesting (EH) device, which essentially depends on the conversion medium. Planar metamaterials or metasurfaces have been used for RF EH due to their distinctive properties such as negative permittivity, negative permeability and refractive index that are not found in nature [1]–[4]. In the recent advances made in power electronics and wireless technology, wireless sensor applications in various scenarios are being developed. The wireless nature of these systems makes it necessary to have a provision for self-powered devices.

Currently, batteries have still been the essential power source for these system devices, but this way has many intrinsic drawbacks, such as the size of the battery, total weight, limited battery life, replacement of batteries for larger number of sensors, and the cost of these devices. For these reasons, there are increasing efforts to develop new power sources to meet the energy needs of these wireless sensor systems. Alternative approaches to this challenge are delivering the power wirelessly from a source or using EH from surrounding ambient sources in an efficient way.

The concept of EH is thus the mechanism of capturing the energy from surrounding ambient sources such as human power, vibrations, thermal and solar energy into usable electric power [5]. In general, the EH process can be seen in Fig. 1. EH is a complex process, because the amount of power harvested from the ambient environment is usually small

The associate editor coordinating the review of this manuscript and approving it for publication was Davide Comite.

TABLE 1. Available ambient energy sources [13]–[17].

Sources	Solar Energy	Thermal Energy	RF Energy	Piezoelectric Energy	
				Vibration	Push Button
Power Density	100 mW/cm^2 (direct sunlight) [14]	100 μW/cm^2	0.1 μW/cm^2-GSM 1 μW/cm^2-Wi-Fi [17]	200 μW/cm^2 [14]	50 μJ/N
Output	0.5 V (single Si cell) 1.0 V (single a-Si cell)	-	3–4 V (open circuit)	10–25 V	100–10,000 V
Available Time	Daytime (4–8 hrs)	Continuous	Continuous	Activity dependent	Activity dependent
Pros	Large amount of energy	Always available	Omnipresent energy	Well-developed technology	Well-developed technology
Cons	- Need large area - Orientation issue	- Need large panel area - Lower power	Distance dependent	Need large area	Highly variable output

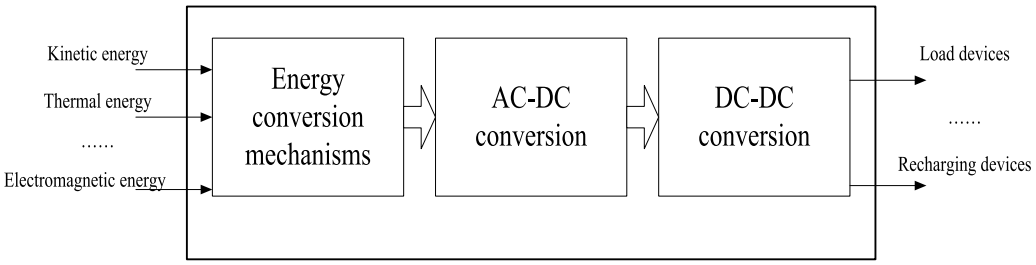

FIGURE 1. Schematic outline of generalized EH process [12].

and the output power is always AC voltage which needs to be converted to DC voltage to power low-power electronic devices or recharge batteries. An EH system can comprise solar energy, thermal energy, piezoelectric energy and RF energy, in which most suitable/conductive mechanisms are practiced to convert those environmental energies into useful electrical energy. Among them, RF energy is omnipresent energy in space due to the abundant availability of EM signals such as television/digital television (TV/DTV) [6], mobile stations [7], [8], and Wi-Fi signals [9]–[11]. The RF EH system has two important units, a receiving antenna and a rectifier circuit, that are responsible for capturing and converting the RF power into usable DC energy.

Conversion efficiency is a highly significant parameter that determines the performance of the harvesting mechanism and relies highly on the conversion medium. In practice, to achieve high conversion efficiency, the EH device should be highly adjusted to its power source [12]. Therefore, this paper introduces the overview of RF EH systems in Section II. The fundamentals of metasurfaces are outlined in Section III. In addition, comparisons of the reviewed metasurface antenna/rectenna designs are presented in Section IV and eventually will be summarized in Section V.

II. OVERVIEW OF RF EH

A. ENERGY SOURCES IN AMBIENT ENVIRONMENT

There are many ambient sources for EH, such as light, thermal gradients, sound energy, wind energy, and RF energy. Some potential ambient energy sources have been summarized in Table 1.

In comparison with solar, thermal, and piezoelectric energies, RF energy is available continuously for both indoor and outdoor environments throughout the day/night due to cell phone towers, satellites, radar stations, Wi-Fi routers, and other wireless devices/communication networks. The typical design of the RF EH network is described in Fig. 2. It consists of three main parts: information gateways, RF energy sources, and network devices. The RF sources are categorized into types: dedicated RF sources and ambient RF sources [6].

The dedicated RF sources can use the license-free ISM frequency bands for RF EH/RF power transfer and provide energy when a more predictable energy supply is needed. The ambient RF sources have various power levels, from

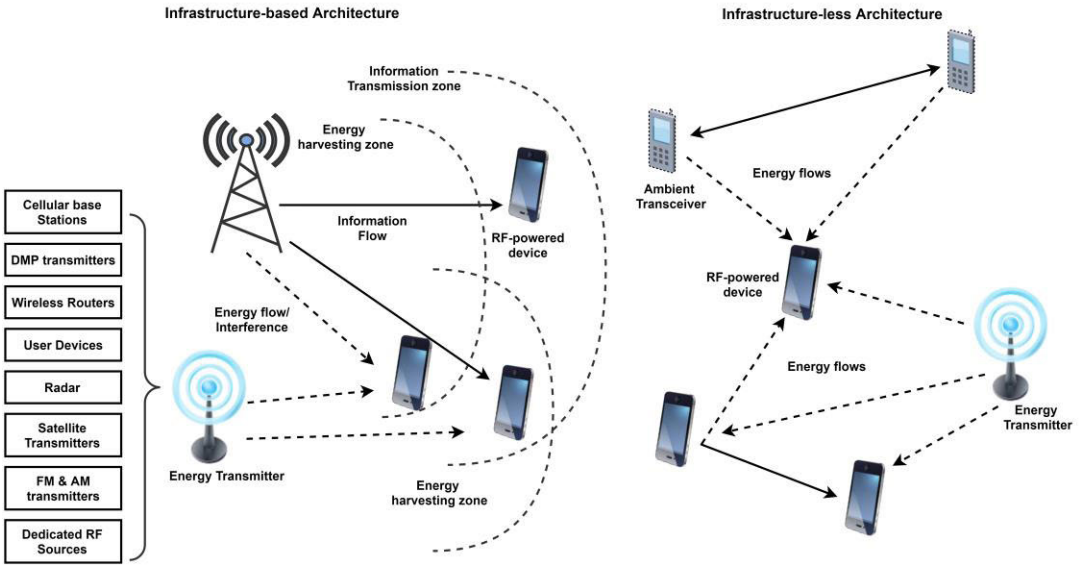

FIGURE 2. Illustration of general structure network of RF EH [18].

around 10 W for cellular and RFID systems, 10^6 W for TV towers, and to roughly 0.1 W for mobile communication devices/Wi-Fi systems [18].

The amount of energy that can be captured in RF EH depends on the transmit power, wavelength of the RF signal and distance between RF energy source and harvesting node. For a transmitter-receiver antenna in free space where there is only one single path between a transmitter and a receiver, the harvested power at the receiving antenna can be calculated based on the Friis equation [19] as follows:

$$P_R = P_T \frac{G_T G_R \lambda^2}{(4\pi d)^2 L} \tag{1}$$

where P_R is the power at the receiver antenna, P_T is the power at the transmitter antenna, L is the path loss factor, G_T is the transmitter antenna gain, G_R is the receiver antenna gain, λ is the wavelength of the RF signal, and d is the distance between the transmitter antenna and the receiver antenna. However, the receiver antenna may capture the RF signal from the transmitter antenna from multiple paths due to RF scattering and reflection. So, the harvested power at the receiver antenna can be calculated by considering the received RF signal through the line-of-sight path and the reflected path separately, as given in (2).

$$P_R = P_T \frac{G_T G_R h_t^2 h_r^2}{d^4 L} \tag{2}$$

where h_t and h_r are the heights of the transmitter and receiver antennas, respectively.

B. RF EH SYSTEM

In an RF EH system, a rectenna is the main harvesting device which can be used to scavenge the RF power. The rectenna system contains three parts: receiving antenna, matching network, and rectifier circuit [20], as shown in Fig. 3.

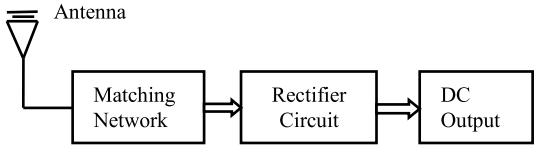

FIGURE 3. Schematic of general structure of rectenna system.

1) ANTENNA DESIGN

A receiving antenna is an essential part of a rectenna system and is strongly effective in conversion efficiency. The antenna can be optimized to resonate at single or multiple frequency bands which are used to capture electromagnetic (EM) waves from the ambient RF sources. For larger power device applications, high gain receiving antennas are needed to harvest enough energy.

Various types of conventional antennas with different structures, such as microstrip antennas [21], monopole antennas [22], dipole antennas [23], and ring-slot antennas [24], [25], are used in RF EH applications to achieve long-distance microwave wireless power transmission (WPT). In [26], a receiving broadband slot antenna fed by a ground coplanar waveguide with high gain was designed. The grounded coplanar waveguide is combined with a rectifier circuit to improve rectenna efficiency. A 1×4 patch antenna array with optimized excitation distribution was designed in [27] with enhanced bandwidth for RF EH applications. The antenna array is combined with a higher efficiency rectifier. A dual-band antenna was designed at GSM 1900 and UMTS-band to harvest energy in an urban environment [28]. An array of rectangular patch antennas with 16 elements was designed to achieve a high amount of EM waves for WPT application [29]. In [30], a dual-band antenna was designed at Wi-Fi band (2.4 GHz and 5 GHz).

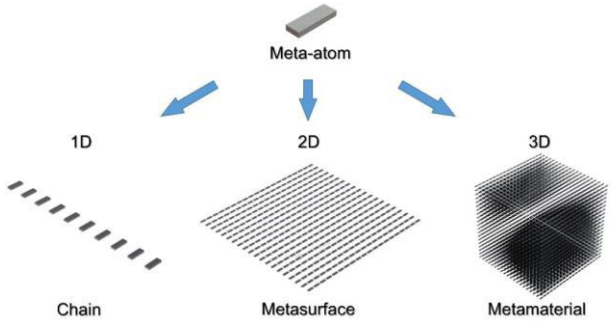

FIGURE 4. Illustration of meta-atom patterns, 1D chain, 2D metasurface and 3D metamaterials [70].

To capture a large amount of power from the ambient environment, which is required in some EH applications, the energy collectors are usually designed in array form. On the other hand, the physical area of the device constrains the overall footprint of the array. Therefore, the EH efficiency can be significantly affected by the size and total number of collectors. In comparison, conventional antennas with large dimensions which are practically identical to half guided wavelength force certain restrictions on utilizing conventional antennas in an array form structure as energy collectors. Furthermore, a distance of more than $\lambda/2$ between the antennas elements is required to avoid destructive mutual coupling in the antenna array [31]. In addition, antenna element coupling, the difficulty in feeding network design, and high loss of array feeding are constraints which cause reduced performance of rectenna arrays. Therefore, the metasurface-inspired rectenna design method has been investigated to overcome these challenges. The metasurface-based energy harvesting antennas/rectennas are discussed in detail in the paper.

2) MATCHING NETWORK

The impedance-matching network is a resonator circuit operating at the designed frequency to maximize the input voltage of a rectifier circuit by reducing the transmission loss between an antenna and a rectifier circuit [32]. This maximizing can be achieved when the impedance at the antenna output is conjugated to the impedance of the load. The matching network is usually made of reactive components such as coils, resistors, and capacitors. Now, there are three matching networks designed for RF EH, i.e., transformer, shunt inductor, and LC network [33].

3) RECTIFIER CIRCUIT

The rectifier circuit is used to convert the RF signals captured by a receiving antenna into DC voltage. The key challenge of the rectifier design is to generate a DC voltage from low-power RF input. Generally, to get higher conversion efficiency, diodes with lower built-in voltage were used. Basically, the three main options for a rectifier are a diode [34], a bridge of diodes [35], and a voltage rectifier-multiplier [36].

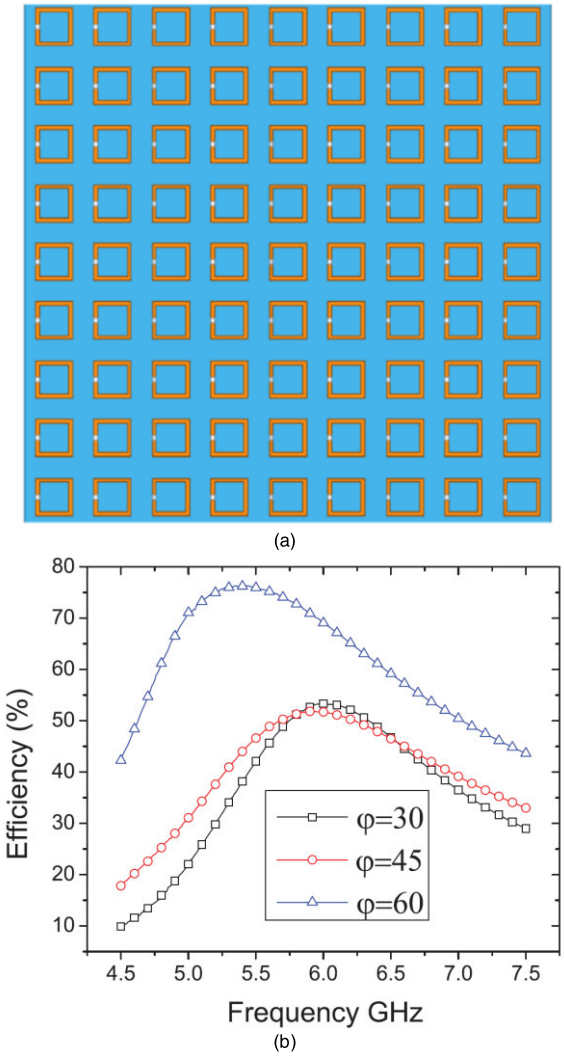

FIGURE 5. (a) Schematic of 9 × 9 SRR metasurface; (b) power efficiency of 9 × 9 SRR metasurface in three different phases [87].

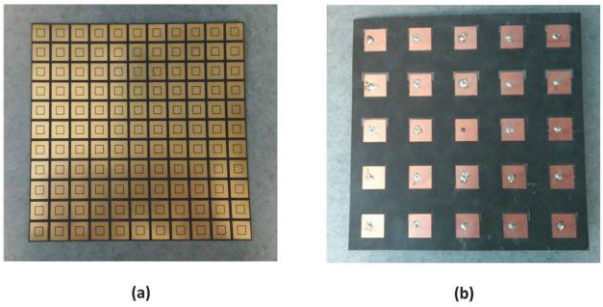

FIGURE 6. (a) Front view of fabricated G-CSRR array and (b) microstrip patch antenna array [88].

The main component of the rectifier circuit is a diode which determines the performance of the rectification circuitry. The rectification circuitry performance usually depends on the saturation current, junction capacitance and its conduction

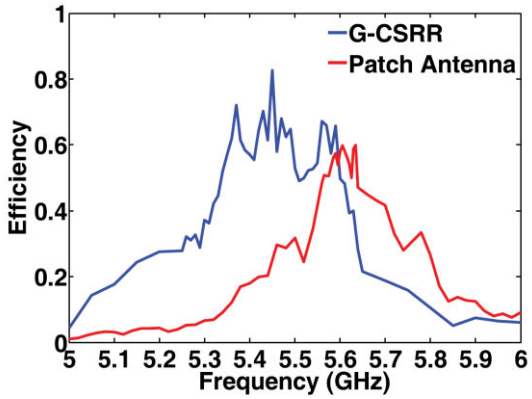

FIGURE 7. Power conversion efficiency of central unit cell for G-CSRR and microstrip patch antenna [88].

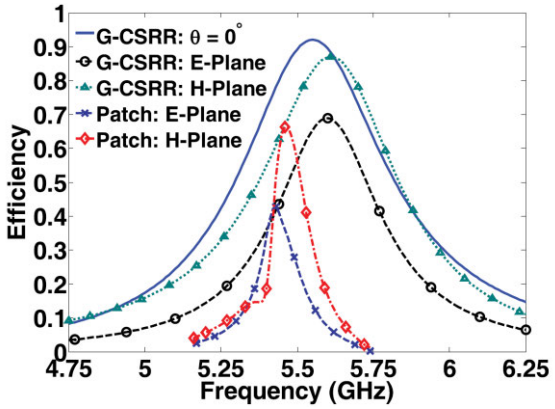

FIGURE 8. Power efficiency of G-CSRR array and microstrip patch antenna array at $\varphi = 60°$ [88].

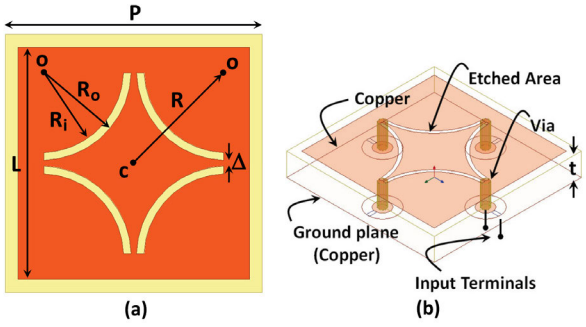

FIGURE 9. (a) Illustration of top view of WG-CSRR cell. (b) Geometry of WG-CSRR resonator [90].

resistance of the diode. The most commonly used diode for the rectifier circuit is the Schottky barrier diode [18].

III. FUNDAMENTALS OF METASURFACES

Recently, metamaterials/metasurfaces have attracted an extraordinary consideration because of their excellent properties that are not found in nature. Metamaterials are novel manufactured materials that are made out of periodic sub-wavelength metal/dielectric structures that can be developed

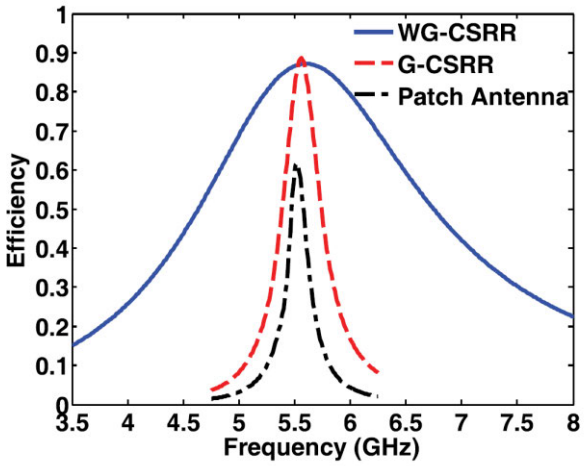

FIGURE 10. Comparison of power efficiency for WG-CSRR array [90] and G-CSRR array and microstrip patch antenna (both reported in [88]).

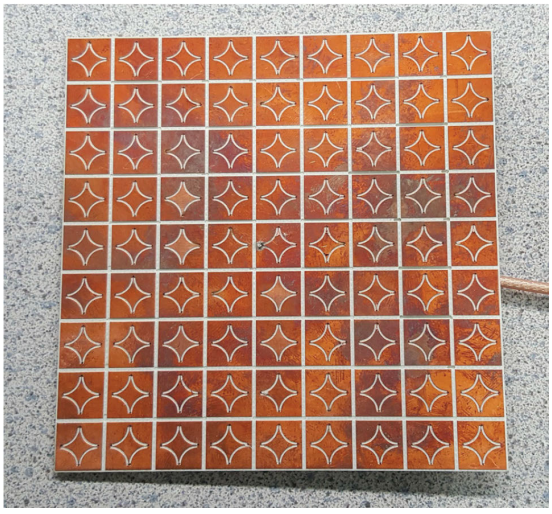

FIGURE 11. Front view of fabricated 9 × 9 WG-CSRR array [90].

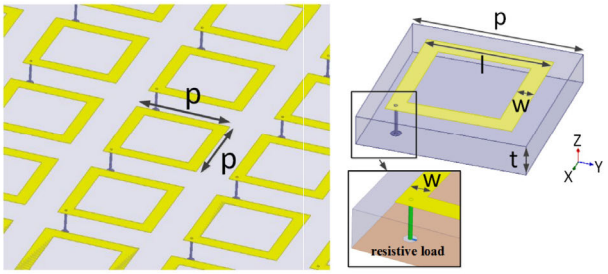

FIGURE 12. Schematic of proposed metasurface harvester [91].

to achieve a strong coupling to both ingredients of incident EM fields (electric and magnetic) [4], [37]–[42]. The unique properties of metamaterials such as negative permittivity, negative permeability, and refractive index make it more attractive to use in EM applications at frequencies ranging

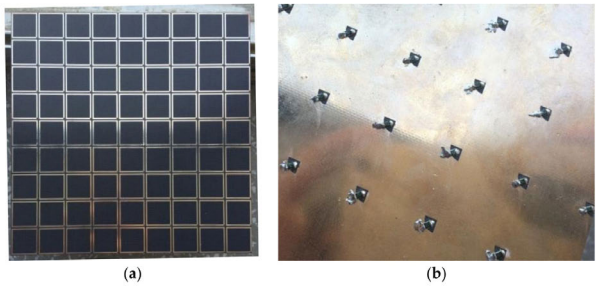

FIGURE 13. Fabricated metasurface array: (a) front view and (b) back view [91].

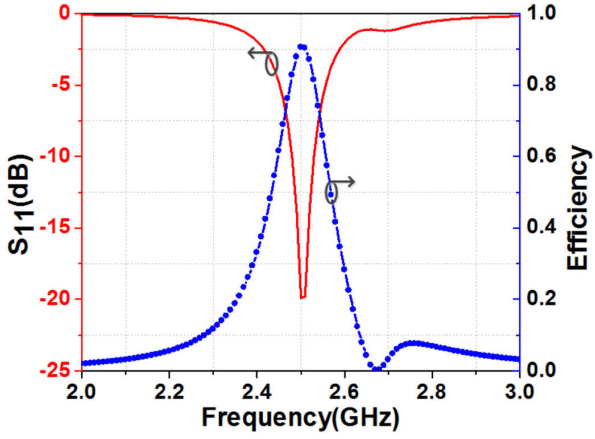

FIGURE 14. Reflection coefficient and harvesting efficiency of metasurface harvester [91].

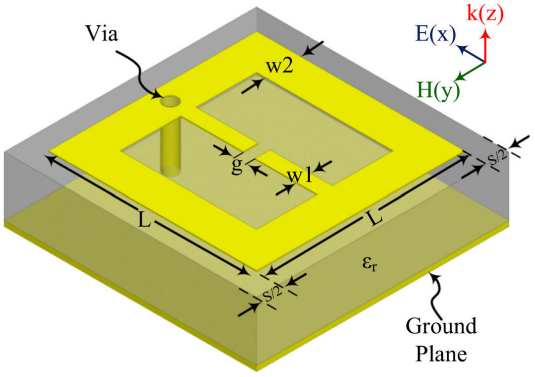

FIGURE 15. Schematic of proposed unit cell (ELC) [92].

from low microwave to optical including cloaking [43], [44], perfect absorber [45]–[51] and RF EH systems [52]–[64]. These are promising applications, but the high losses and strong dispersion associated with resonant responses prevent the use metamaterials in practice. Also, the difficulty in micro- and nano-fabrication required to manufacture the three-dimensional structures is another challenge of metamaterials/metasurfaces [65]. Planar metamaterials are widely accessible in the optical regime and can be smoothly fabricated using some nano-printing and lithography techniques.

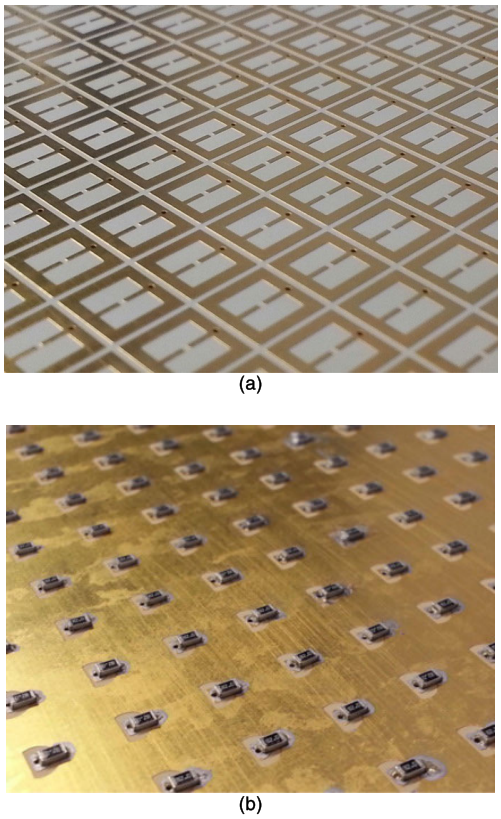

FIGURE 16. Fabricated 13 × 13 array: (a) front view and (b) back view [92].

These features have driven many researchers to concentrate on a single layer of planar metamaterial [66]. These planar materials are known as metasurfaces and can be counted as the two-dimensional (2D) counterparts of metamaterials [67]–[69].

A metasurface is an artificial material made of an array of unit cell structures, as shown in Fig. 4.

Due to their small losses, and low profile, metasurfaces are able to manipulate the EM waves at subwavelength propagation distances with more complicated applications such as generalized refraction, polarization transformation and signal multiplexing [71], [72]. The EM waves in a metasurface propagate differently in the homogenous medium and have three unique properties: extremely short wavelength, abrupt phase change and chromatic dispersion. These unique properties identify the propagation waves in a metasurface from those waves in natural materials and metamaterials. The metasurface changes the EM waves essentially by exploiting the boundary conditions while 3-dimensional materials change EM waves depending on the constitutive parameters [73]. The boundary conditions depend on the continuous tangential components of electric and magnetic fields across an interface between two dielectric media. Due to their rich EM field manipulation capabilities, metasurfaces could enable many incredible applications in the field of optics and nanophotonics, such as shielding [74]–[76], EH [57], [77]–[83], antennas [84]–[86], radomes, etc.

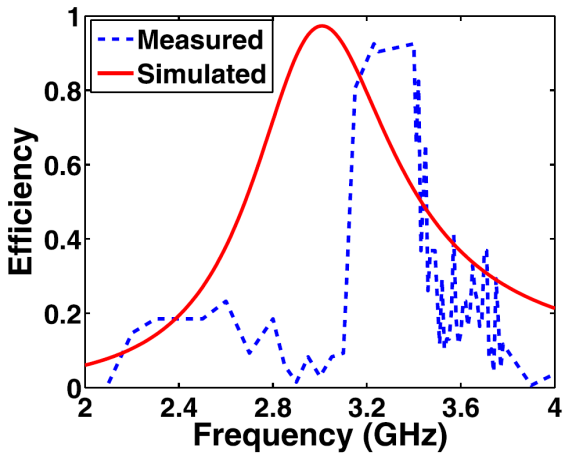

FIGURE 17. Simulated and measured efficiency of harvester [92].

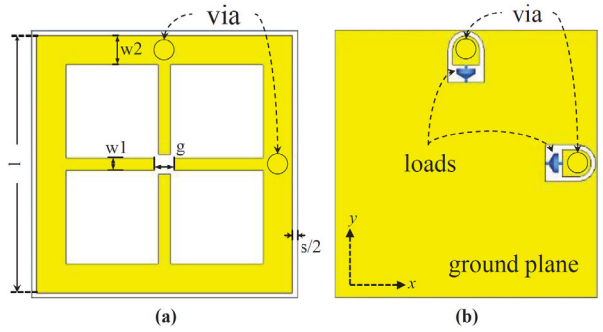

FIGURE 18. Schematic of symmetric ELC resonator harvester: (a) top view; (b) bottom view.

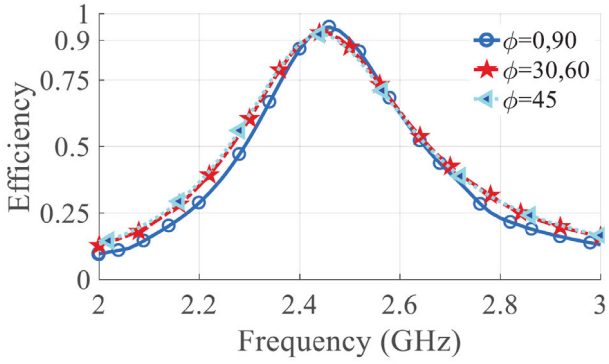

FIGURE 19. Simulated power efficiency of ELC resonator for different polarization angles [93].

IV. RF EH ANTENNA/RECTENNA USING METAMATERIAL/METASURFACE STRUCTURES

RF EH antennas/rectennas are an attractive research field right now due to the recent demand of many power devices/electronic sensors. In this section, we first describe metasurface-based antennas for RF EH and review the existing research of metasurface antennas in this field. Then, metasurface-based rectennas for RF EH are reviewed and discussed.

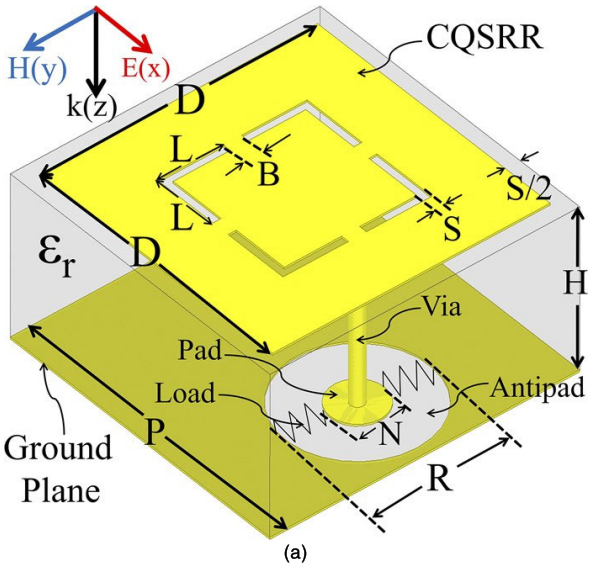

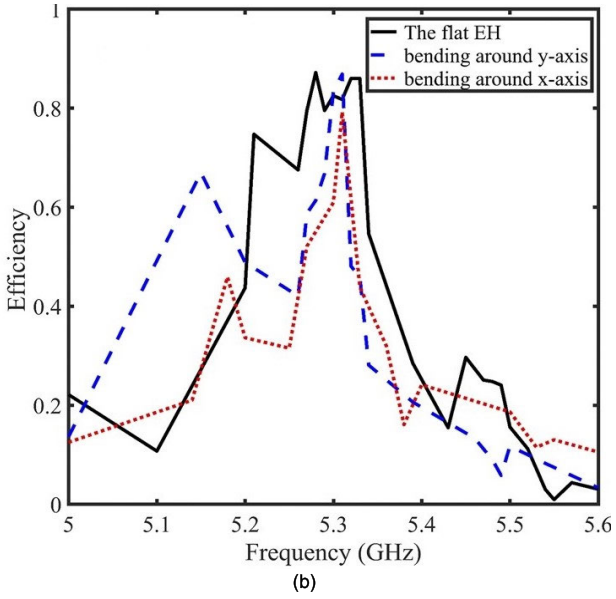

FIGURE 20. (a) Illustration of proposed metasurface unit cell. (b) Measurement efficiency of flat and curved EH under normal incident [94].

A. METASURFACE-BASED ANTENNA FOR RF EH

WPT and EM/RF EH indicate to capture the energy of EM waves from the surrounding ambient environment using a rectenna (receiving antenna with rectifying circuit) system. The overall power conversion efficiency of the rectenna system basically relies upon the efficiency of the antenna, which is the main collector of EM waves. For EH applications, higher efficiency collectors are desired; as a result, using metamaterial cells as EM collectors has grown in popularity. In metamaterial absorbers, the surface impedance should match the free space impedance to achieve a full absorption and improve EH efficiency. In contrast to the absorbers, the meta-harvester absorbs the incident EM wave energy and channels it to the load. Meta-harvesters were built on

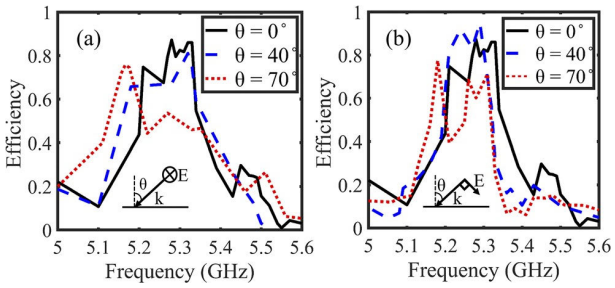

FIGURE 21. Measured efficiency of flat harvester at different incident angles: (a) TE mode and (b) TM mode [94].

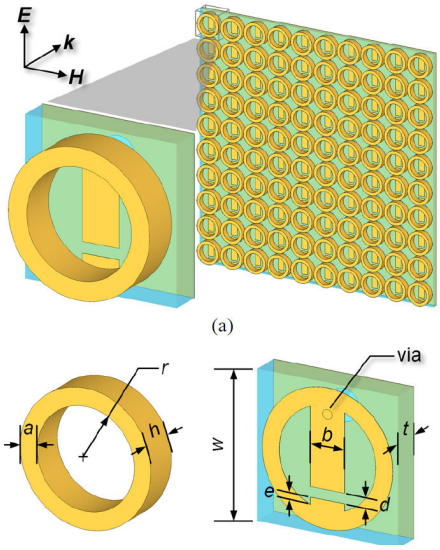

FIGURE 22. Schematic of proposed metamaterial unit cell; (a) periodic array [95].

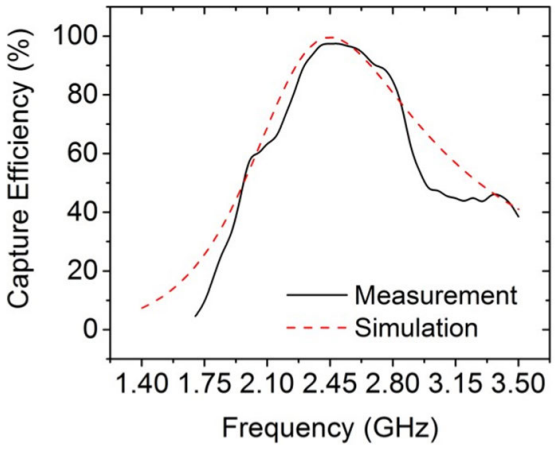

FIGURE 23. Simulated and measured captured efficiency under normal incident [95].

two common structures of split-ring resonators (SRRs) [87] and complementary split-ring resonators (CSRRs) [88], [89]. The SRR is one resonator that attracted the researchers and consists of one or multiple broken loops where the loops are engineered concentrically.

In [87], SRRs have been designed by using thin traces of microstrip lines at 5.8 GHz, as shown in Fig. 5(a). The primary objective of this work is to demonstrate the feasibility of the SRR resonator by gathering the captured power equivalent AC with high conversion efficiency in the resistive load located in the gap of each unit cell. The ratio of total power incident on the surface to the available power at the feed of the AC-to-DC interface is known as the RF-DC conversion power efficiency. The efficiency is more than 40% for three different incident angles (30°, 45°, 60°) with bandwidth of 1.5 GHz, as shown in Fig. 5(b).

The comparison in terms of power harvesting efficiency and bandwidth for a ground-backed CSRR (G-CSRR) array and patch antenna array has been presented in [88]. A 11×11 array of G-CSRR resonators and 5×5 patch antenna array were designed at 5.55 GHz as depicted in Fig. 6. To compare the power efficiency, the delivered power to load of the central cell of each G-CSRR array and microstrip patch antenna was measured. The power efficiency was observed to be 83% for the G-CSRR cell at the resonant frequency and 60% for the patch antenna, which is 23% smaller than for the G-CSRR cell, as shown in Fig. 7, due to the strong resonance and coupling between the unit cells, which enhances its constitutive parameters and filtering characteristics. The G-CSRR array shows a wider half-power bandwidth (HPBW) than that of the patch antenna array at an oblique incident of in H-plane and E-plane excitations, as illustrated in Fig. 8.

An array of wideband G-SCRRs (WG-CSRRs) inspired by chaotic bow-tie cavities has been designed for EM EH [90]. A bow-tie cavity consists of four perfectly electric conducting cylinder handles on a dielectric substrate as seen in Fig. 9. Fig. 9(b) represents the WG-CSRR cell with four vias to gather and deliver the power on the bridge that is created by the etched area. The WG-CSRR resonator shows 87% power efficiency at the resonance frequency, which is analogous to that of the G-CSRR array [88]. This is comparable to that of the G-CSRR array, with an advance of almost 4.5 times in the bandwidth of the WG-CSRR array, as shown in Fig. 10.

A 9×9 WG-CSRR unit cell based array has been fabricated to verify the value of the frequency bandwidth enhancement, as shown in Fig. 11.

A wideband, polarization-insensitive metasurface EH was built in [91] at 2.5 GHz (LTE/Wi-Fi). The metasurface unit cell involved a subwavelength electrical small square-ring resonator, as shown in Fig. 12.

The size of the metasurface unit cell is 15.7 mm $\times$ 15.7 mm, and a 9×9 unit cell based metasurface has been designed as shown in Fig. 13 to achieve more than 80% power conversion efficiency, as depicted in Fig. 14.

An array of 13×13 electrically small resonators was constructed in [92] for EM EH. Maximizing the radiation to AC power efficiency is the main goal of the work. The harvester was designed based on an array of ELC (electric inductive–capacitive) resonators at 3 GHz. The proposed unit

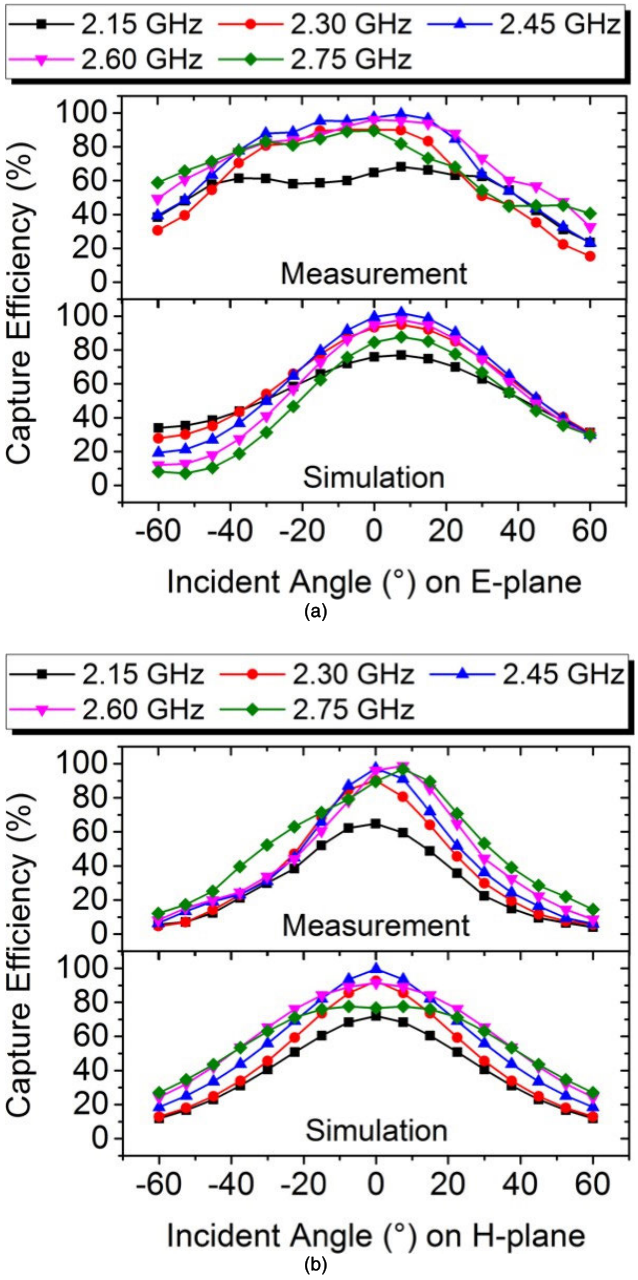

FIGURE 24. Measured and simulated captured efficiency under oblique incident on (a) E-plane and (b) H-plane [95].

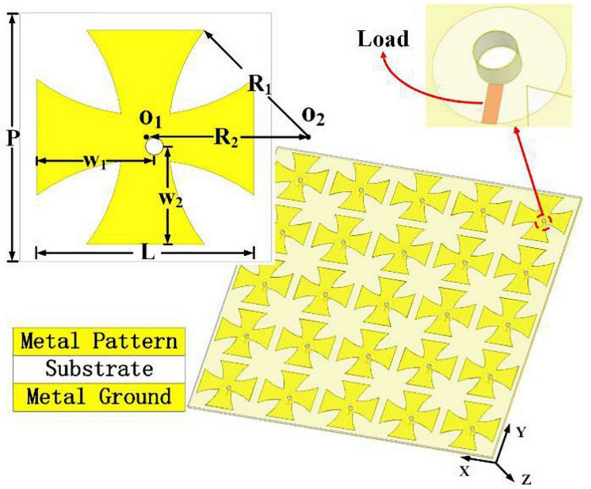

FIGURE 25. Exploded view of proposed metasurface harvester [96].

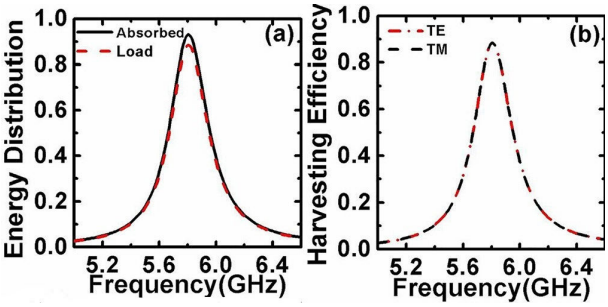

FIGURE 26. Simulated energy distribution and harvesting efficiency for TE and TM modes at normal incident [96].

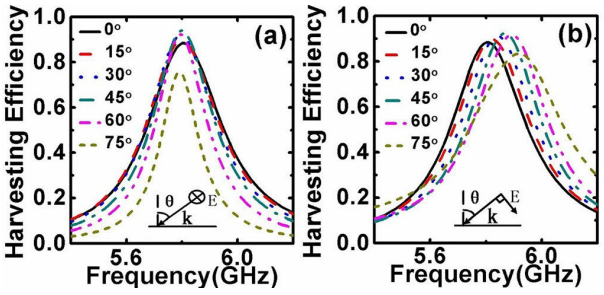

FIGURE 27. Simulated harvesting efficiency at various incident angles: (a) TE mode and (b) TM mode [96].

cell (ELC) contains two face-to-face split rings sharing the same gap handle on the dielectric substrate and ground plane, as illustrated in Fig. 15.

The top and bottom conductive layers are connected by the load through via/probe. Fig. 16 shows the 13 × 13 fabricated unit cells where the distance between two elements is equal to 0.25 mm, and each unit cell has been loaded with an 82 Ω resistor, as depicted in Fig. 16(b).

The measured power efficiency of 93% was observed, while the simulation yielded 97%, as shown in Fig. 17.

A metasurface based on 9 × 9 symmetric ELC resonator unit cells with polarization-independent characteristics was designed at 2.45 GHz for EH application [93]. The proposed ELC resonator is very insensitive to the polarization of the incident wave and has two vias loaded with two resistors, as shown in Fig. 18.

Fig. 19 shows that an efficiency of more than 92% has been achieved for different polarization angles (0° to 90°).

In [94], a flexible ultra-thin curvature metasurface-based EH system was designed at 5.33 GHz. The presented harvester consists of a complementary quad SRR (CQSRR) handle on the substrate material of Rogers RO3010 PCB ($\varepsilon_r = 10.2$ and $\tan\delta = 0.0022$) with a thickness of 254 μm and surrounded by a copper layer as a bottom layer.

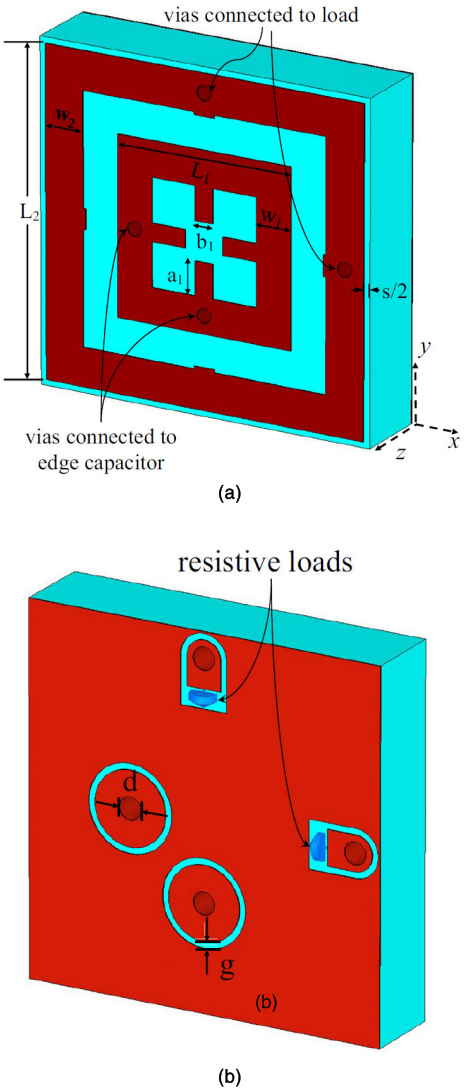

FIGURE 28. Geometry of proposed unit cell: (a) top view and (b) bottom view [97].

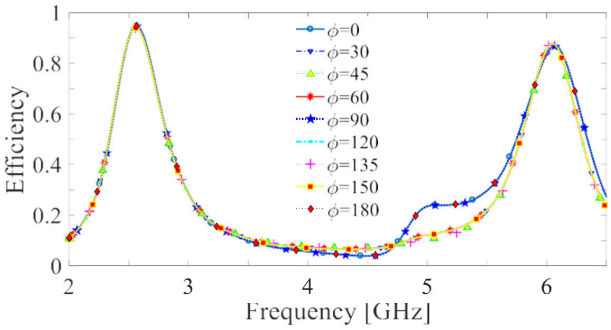

FIGURE 29. Harvesting efficiency of harvester under different polarization angles [97].

The cell is loaded by two parallel lump resistors of 100 Ω in a bottom layer using a via/probe as illustrated in Fig. 20(a). Fig. 20(b) shows the efficiency of flat and curved harvesters under the normal incident. At the normal incident,

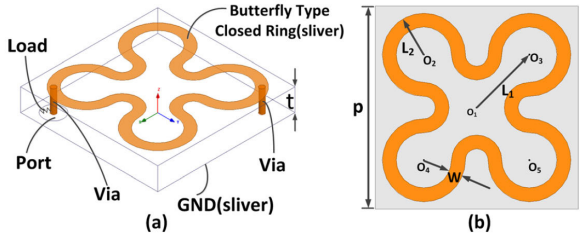

FIGURE 30. Schematic of proposed BCR unit cell: (a) solid view and (b) top view [98].

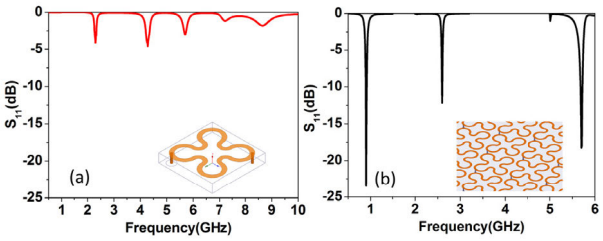

FIGURE 31. Return loss: (a) BCR single unit cell and (b) BCR periodic array [98].

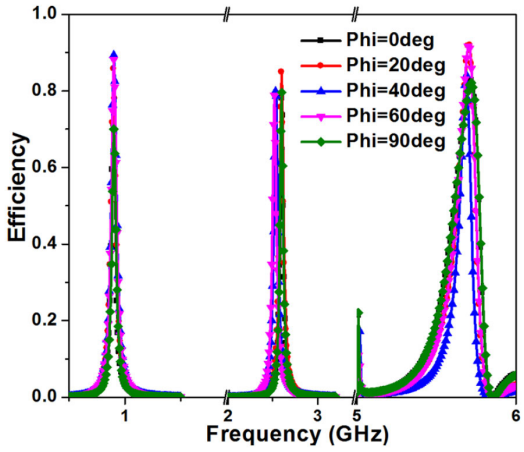

FIGURE 32. Power efficiencies of BCR array for various polarization angles under normal incidence [98].

the efficiency (HPBW) of the flat energy harvester is 0.86 (0.053) while the harvester achieved 0.72 (0.091) and 0.62 (0.036) efficiency at the oblique incident 70° for H-plane and E-plane, respectively, as shown in Fig. 21.

A metamaterial EH with wideband reception, high capture efficiency and wide incident angle was presented at 2.45 GHz [95]. The harvester consists of 10×10 resonators comprising metallic mirrored split rings with hollow cylinders as illustrated in Fig. 22.

The 90%-efficiency bandwidth is achieved by lowering the resonator's quality factor using the hollow cylinder. The harvester achieved capture efficiency up to 97% at the resonance frequency and a relative bandwidth of 16% with efficiencies above 90% across a frequency range from 2.3 to 2.7 GHz, as shown in Fig. 23 and Fig. 24.

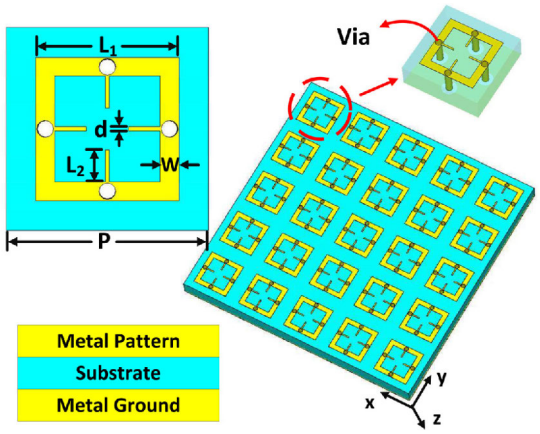

FIGURE 33. Geometry of proposed metamaterial array and its unit cell [99].

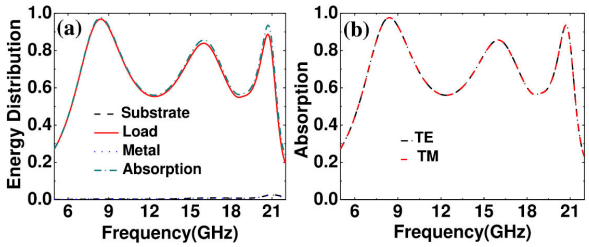

FIGURE 34. (a) Power distribution efficiency and (b) absorption efficiency on the normal incident for TE and TM [99].

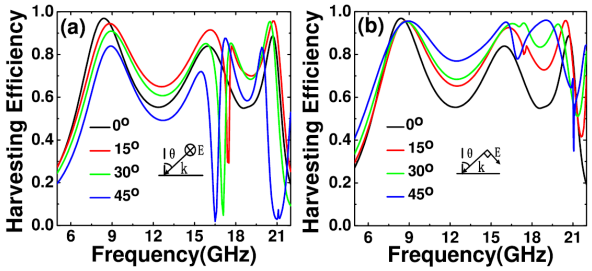

FIGURE 35. Measured harvesting efficiency at different incident angles: (a) TE mode and (b) TM mode [99].

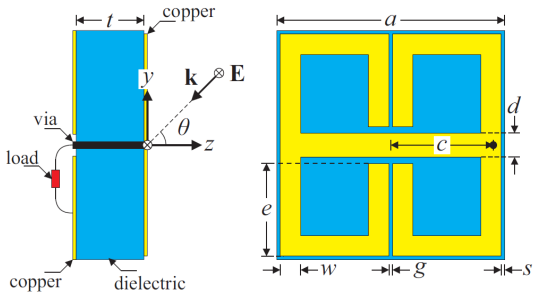

FIGURE 36. Schematic of proposed meta-harvester unit cell [100].

A wide-angle, polarization-insensitive metasurface harvester was designed in [96]. The proposed metasurface unit cell has the shape of rotating central symmetry with only one

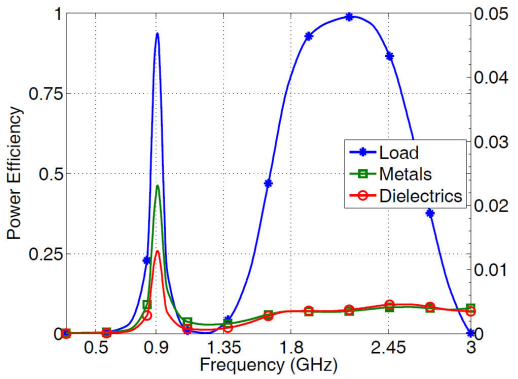

FIGURE 37. Simulated power efficiency [100].

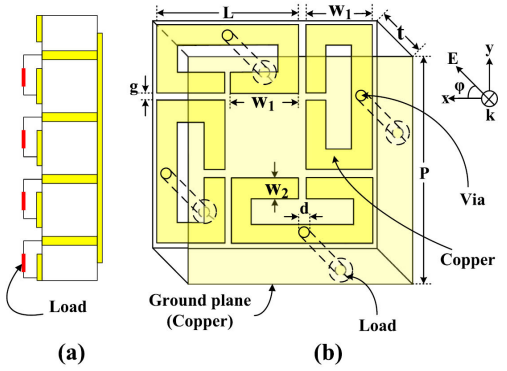

FIGURE 38. Geometry of proposed unit cell [101].

via, as shown in Fig. 25. The simulated harvesting efficiency of 88% was achieved at 5.8 GHz for arbitrary polarization at the normal incident of 0°, as illustrated in Fig. 26, while the maximum harvesting efficiency is 77% in the oblique incident range of 75°, as shown in Fig. 27.

A dual-band and multi-polarization metasurface-based EM EH was presented in [97]. The primary goal of this work is maximizing the harvesting efficiency at the resonance frequencies of 2.4 and 6 GHz. To achieve a high harvesting efficiency, the surface of the proposed unit cell was pixelized, and then a binary optimization algorithm was applied. The proposed unit cell comprises a ring resonator loaded with two resistive loads through two vias and a symmetric ELC resonator loaded with two edge capacitors as shown in Fig. 28.

The efficiency of 90% has been achieved at both operating frequencies of 2.45 and 6 GHz, as illustrated in Fig. 29.

An array of a 7 × 7 butterfly-shaped closed-ring (BCR) unit cell based metasurfaces was designed in [98] for an EH system. The wide-angle, polarization-insensitive harvester can collect energy from the ambient environment and then deliver it to the load through one port at three bands of 0.9, 2.6, and 5.7 GHz. The BCR unit cell is built with two vias; one is connected to the load of the collecting port while the other via is connected to the resonator and ground to minimize the

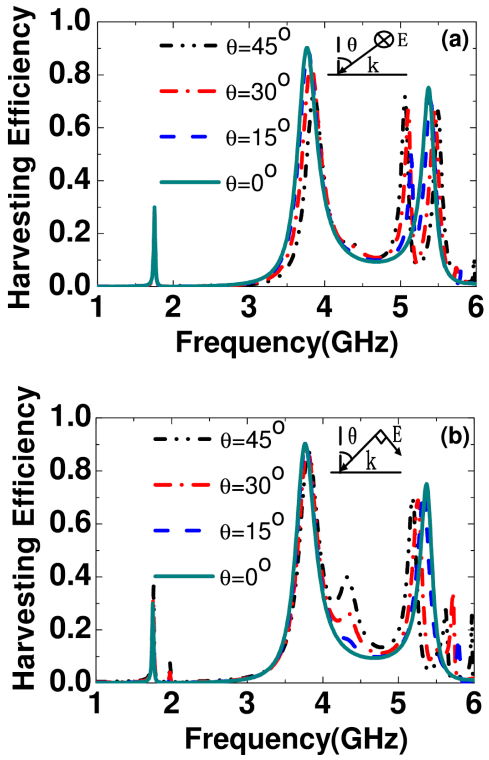

FIGURE 39. Measured harvesting efficiency at various incident angles: (a) TE polarization and (b) TM polarization [101].

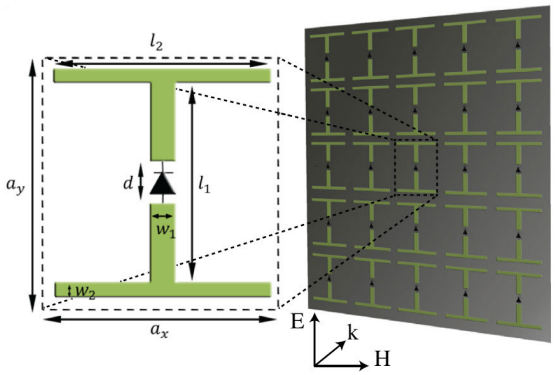

FIGURE 40. Illustration of metasurface energy harvester [103].

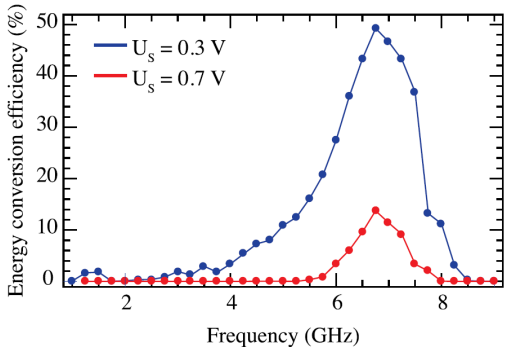

FIGURE 41. Power conversion efficiency for different values of diode threshold voltage [103].

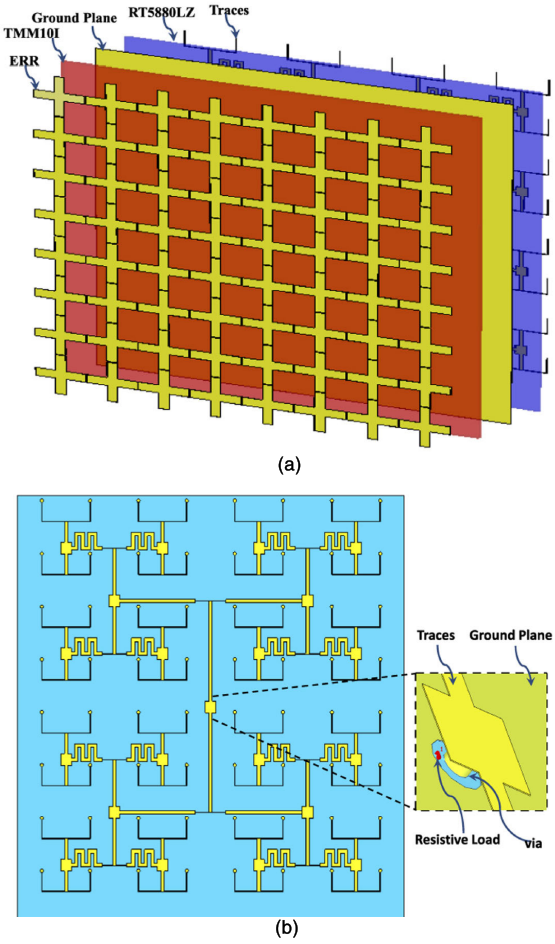

FIGURE 42. (a) Schematic of harvester array and (b) corporate fed network [104].

structure of the unit cell by increasing the inductance value of the resonant structure, as illustrated in Fig. 30.

The comparison of the simulated return losses of the single unit cell and periodic array of BCR resonator is shown in Fig. 31, where the resonant frequencies of the BCR unit cell are shifted to higher frequency band with BCR periodic array. As shown in Fig. 32, the conversion power efficiencies are 70%, 80% and 82%, respectively, for 900 MHz, 2.6 GHz and 5.7 GHz.

A wide-angle, polarization-independent, wideband metamaterial array for EH and WPT was designed in [100]. The proposed unit cell comprises one square ring and four metal bars as illustrated in Fig. 33.

The design shows a wide operation bandwidth with HPBW of 110% across the frequency range from 6.2 to 21.4 GHz. For the random polarization wave under the normal incidence, the maximum harvesting efficiency was 96% and the HPBW was 110%.

Maximum efficiency higher than 88% with HPBW more than 83% was achieved at the oblique incident of 45°,

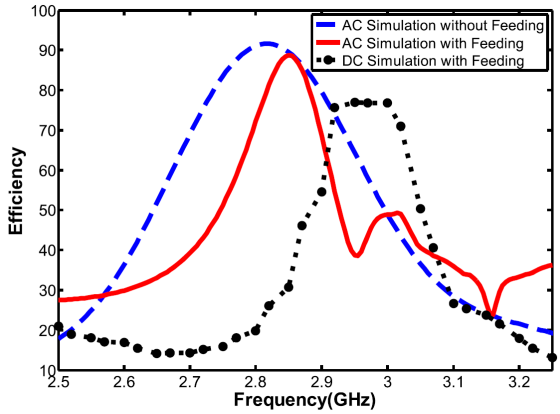

FIGURE 43. Simulated AC power efficiency [104].

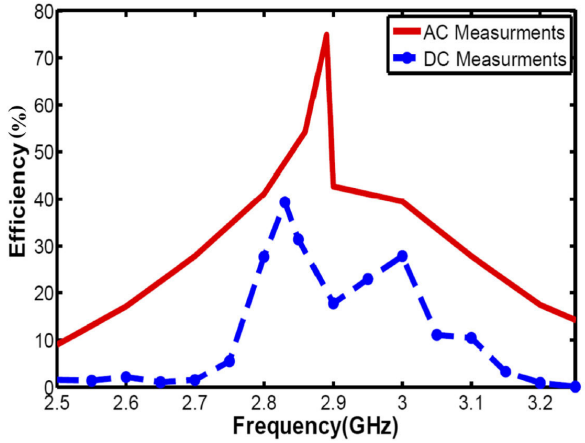

FIGURE 44. Measured AC and DC power conversion efficiencies [104].

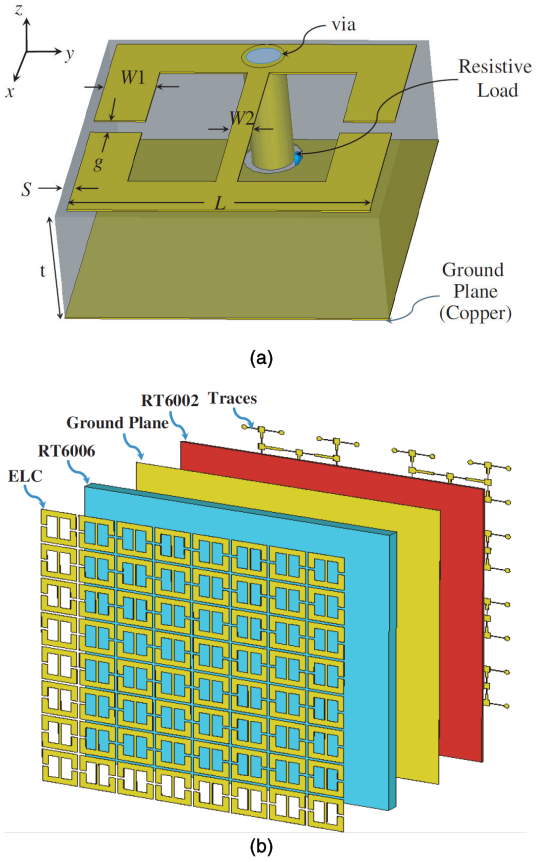

FIGURE 45. (a) Illustration of ELC unit cell and (b) schematic of metasurface harvester [105].

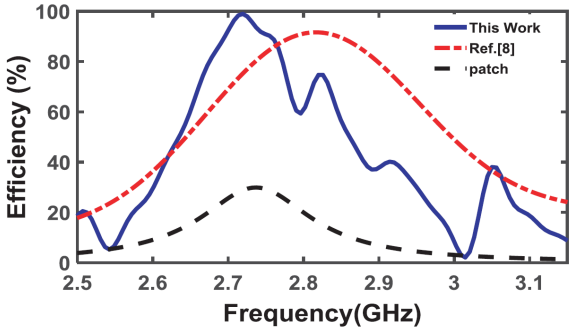

FIGURE 46. Comparison between the simulated AC efficiency for metasurface [105] and patch antenna/metasurface [104].

as shown in Fig. 34 and Fig. 35, respectively. The disadvantage of this design is the use of four vias to deliver the absorbed power to the load, which means more complexity and more loss. The absorption efficiencies on the normal incidence are 97%, 87%, and 93%, respectively, at 8.4, 16 and 20.7 GHz.

A highly efficient, wide-angle, triple-band (0.9 GHz, 1.8 GHz, Wi-Fi) metamaterial harvester has been presented in [101]. The proposed harvester is an array of ELC resonators that can collect the energy from the ambient environment then drive it to the optimal load by a via as illustrated in Fig. 36. The simulated results show that the power efficiency is more than 94% and 98% at 0.9 and 2.2 GHz, respectively, and 81% and 87% for 1.8 and 2.45 GHz, respectively, as shown in Fig. 37.

A 7 × 7 metamaterial unit cell based metasurface was designed in [102] for a wide-angle, polarization-insensitive EM EH system. The proposed harvester can resonate at triple-band frequencies (GSM 1800, WiMAX, WLAN). The unit cell of the metasurface includes four SRRs arranged in rotating central symmetry, as illustrated in Fig. 38, where each unit cell has four vias to channel the power to the loads. The measured results show that the harvesting efficiencies are 26%, 88%, and 72%, respectively, at 1.7, 3.7, and 5.2 GHz, as shown in Fig. 39.

The metasurface harvester for RF EH mentioned above only distributes the collected power in each metasurface unit cell array without rectification circuitry. The metasurface harvesters for RF EH have developed from a single-band to wideband or multi-band, from single-polarization to multi-polarization or even wide-angle polarization and polarization-insensitive, so that they could efficiently capture

TABLE 2. Summary of research on planar metamaterial/metasurface structure based antennas/rectennas for RF EH applications.

First author, year	Structure	Substrate material	Dimensions @ Array	Frequency	Efficiency (antenna efficiency)		Remarks
					Simulated	Measured	
H.T. Zhong, 2017 [77]	SRR	Rogers Duroid RT5880	$0.6\lambda_0$ @ 3×3 unit cells	5.4 GHz	92% at 0° 98% at 60° (TM-mode)	89% at 0° 96% at 60° (TM-mode)	- Broadband - Polarization insensitive - Wide-angle reception - Each cell has four vias
Wei Hu, 2019 [81]	ELC	F4B/air	$0.6\lambda_0$ @ 8×8 unit cells	2.45 GHz	87.6%	84.4%	Dual-layer structure with a thin low-loss material and an air gap
Omar M. Ramahi, 2012 [87]	SRR	Rogers Duroid RT5880	Approximately $0.114\lambda_0$ @ 9×9 unit cells	5.8 GHz	-	75 % at φ = 60°	Sizeable bandwidth (exceeds 1.5 GHz)
Babak Alavikia, 2015 [88]	G-CSRR and microstrip patch antenna	Rogers Duroid RT5880	$0.34\lambda_0$ @ 11×11 array of G-CSRR and 5×5 array microstrip patch antenna	5.55 GHz	92% for G-CSRR	83% for G-CSRR and 60% for microstrip patch antenna	The G-CSRR has a wider HPBW than that of the microstrip patch antenna
Babak Alavikia 2015 [90]	WG-CSRR inspired by chaotic bow-tie cavities	Rogers RO4003	Approximately $\lambda_0/5$ @ 9×9 unit cells	5.6 GHz	87%	-	- Increases the bandwidth - Four vias to drive power to the load (more complex)
Xuanming Zhang 2018 [91]	electrical small square-ring resonator	F4B	Approximately $0.131\lambda_0$ @ 9×9 unit cells	2.5 GHz (LTE/Wi-Fi)	90%	80%	- Wide-angle reception - Polarization insensitive
Thamer S. Almoneef 2015 [92]	ELC	Rogers TMM10i	$0.075\lambda_0$ @ 13×13 unit cells	3 GHz	97%	93%	Ideal for WPT and space solar power (SPS)
Alireza Ghaneizadeh, 2019 [94]	CQSRR	Rogers RO3010 PCB	$0.13\lambda_0$ @ 11×11 unit cells	5.33 GHz (WiFi)	86%	Higher than 80%	Flexible
Xin Duan, 2018 [95]	Metallic mirrored split rings with hollow cylinders	Polytetrafluoroethylene (PTFE)	$0.16\lambda_0$ @ 10×10 unit cells	2.45 GHz	99.5%	97.3%	- Wideband - Enhances 90%-efficiency bandwidth
Fan Yu, 2018 [96]	Rotating central symmetry structure	-	$0.323\lambda_0$ @ 5×5 unit cells	5.8 GHz	88% at 0° and 77% at 75°	80% at 0° and 68% at 75°	- Wide-angle reception - Polarization insensitive - One via
B. Ghaderi, 2018 [97]	Ring resonator and symmetric ELC resonator	Rogers RT/duroid 6006	$0.093\lambda_{2.45\ GHz}$ @ 9×9 unit cells	2.45 GHz and 6 GHz	Higher than 90%	Close to 90%	- Dual-band - High harvesting efficiency
Xuanming Zhang, 2017 [98]	Butterfly-shaped closed-ring array	F4B	$\lambda_0/12$ @ 7×7 unit cells	900 MHz, 2.6 GHz and 5.7 GHz	70%, 80%, and 82% at 900 MHz, 2.6 GHz and 5.7 GHz, respectively	65%, 70% and 70% at 900 MHz, 2.6 GHz and 5.7 GHz, respectively	- Triple bands - Polarization insensitive - Miniaturized wide-angle reception
H.T. Zhong, 2017 [99]	SRRs	F4B-2	$0.198\lambda_{6.2\ GHz}$ @ 5×5 unit cells	Wideband (6.2–21.4 GHz)	96% at 0° and. 88% at 45°	74% at 0° and 78% at 45°	- Polarization insensitive - Wide-angle reception - HPBW equals 110%
H.T. Zhong, 2016 [101]	Four SRRs arranged in rotating central symmetry	Rogers RO4003	Approximately $0.184\lambda_{1.75\ GHz}$ @ 7×7 unit cells	1.75 GHz, 3.8 GHz, and 5.4 GHz	30%, 90%, and 74% at 1.75 GHz, 3.8 GHz, and 5.4 GHz, respectively	26%, 88%, and 72% at 1.75 GHz, 3.8 GHz, and 5.4 GHz, respectively	- Polarization insensitive - Wide-angle - Each cell has four vias

TABLE 2. ***(Continued.)*** **Summary of research on planar metamaterial/metasurface structure based antennas/rectennas for RF EH applications.**

Bagher Ghaderi, 2018 [102]	ELC resonators	Rogers RT/duroid 6006	Approximately $0.089\lambda_0$ @ 9×9 unit cells	2.45 GHz	Higher than 92%	Higher than 90%	- Polarization insensitive - Two vias in each cell
Gabin T. Oumbé Tékam 2017 [103]	Cut-wire metasurface with integrated PN junction diode	-	Approximately $0.676\lambda_0$	6.75 GHz	50%	-	Uses germanium diode (lower threshold, high bandwidth)

TABLE 3. **Summary of research on metamaterial/metasurface structure based rectennas for RF EH applications.**

First author, year	Structure	Substrate material	Dimensions @ Array	Frequency	AC-DC efficiency (rectenna efficiency)	Remarks
Xin Duan, 2016 [79]	ELC	Rogers RO4450F	$0.612\lambda_0$ @ 6×6 unit cells	2.45 GHz	44.5% at 7 dBm	Super thin profile, easy assembly
Mohamed El Badawe, 2017 [104]	electrical small square-ring resonator	Rogers TMM10i	$0.125\lambda_0$ @ 8×8 unit cells	3 GHz	40% at 12 dBm	Captures power channel to single load using corporate feed network
Mohamed El Badawe 2018 [105]	ELC resonators	Rogers RT6006	$0.068\lambda_0$ @ 8×8 unit cells	2.72 GHz	51% at -2 dBm	Captures power channel to single load
Peng Xu 2016 [106]	SRRs	Rogers 04350 PCB	Approximately $0.127\lambda_0$ @ 8×8 unit cells	2.45 GHz	67% at 10 dBm	Absorbs power channel to single load
Thamer S. Almoneef, 2017 [107]	ELC	Rogers Duroid RT5880	$0.56\lambda_0$ @ 4×4 super cells	2.4 GHz	70% at 9 dBm	Multiple polarization, cell grouping to reduce the feed ports, narrow bandwidth

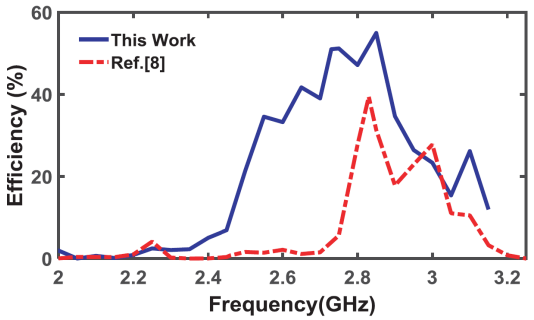

FIGURE 47. **Measured radiation-to-DC efficiency of metasurface harvesters in [104], [105].**

the energy from the ambient RF sources. Table 2 summarizes in detail several configurations of planar metamaterial/metasurface structures that are used in antennas for RF EH applications.

B. METASURFACE-BASED RECTENNA FOR RF EH SYSTEM

In an RF EH system, designing a rectifier circuit with a higher conversion efficiency to generate a DC voltage from the low-input RF signal is challenging. In general, diodes with lower built-in voltage are used, which represents the key factor that affects the performance of the rectification circuitry. The received power density by electrically small elements (metasurface or metamaterial elements) usually is lower than what is required to turn on a rectifying diode. To overcome such challenges, an additional layer is integrated into the metasurface for feeding the network that delivers the harvested energy into a single rectification circuit.

A metasurface EH based on cut-wire unit cells with embedded PN junction diodes was designed in [103], as shown in Fig. 40.

The cut-wire metasurface harvester resonated at 6.75 GHz and is used to capture the energy from ambient sources, in which the electric field is enhanced by an electric dipole resonance while the integrated diode is used for the rectification of the induced current. The simulated power efficiency of 50% for incident power in accord with the typical power of Wi-Fi signals is achieved using a germanium diode ($U_S = 0.3$ V) as illustrated in Fig. 41.

A metasurface harvester based on electrically small resonators has been designed in [104]. The harvester consists of 8×8 array electric ring resonators (ERR) at 3 GHz as shown in Fig. 42.

The harvester array harnesses the EM energy from the ambient environment and collects the absorbed AC power from all array elements to drive it into single-rectifier circuitry using a corporate feed network. The benefit of the proposed metasurface harvester is to maximize the power density per diode and to reduce the number of rectifier circuits, which reduces the fabrication cost and complexity.

Without the corporate feed network, the radiation to AC efficiency is 92%, as shown in Fig. 43. Fig. 44 shows the measured DC efficiency, which is more than 40%. Constructive interference at the rectifier input has resulted in the

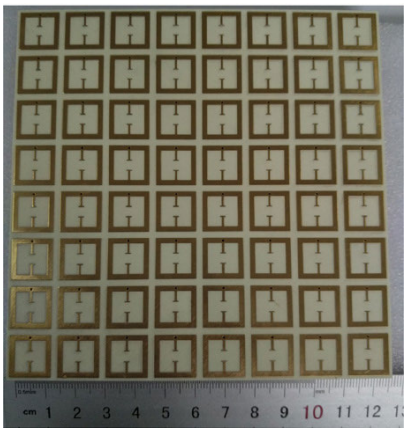

(a)

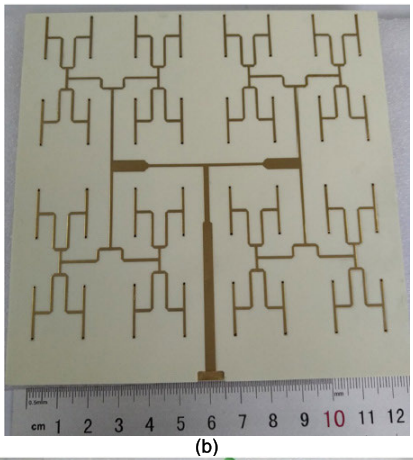

(b)

(c)

FIGURE 48. Fabricated 8 × 8 array harvester: (a) top view, (b) back view, and (c) rectifying circuit [106].

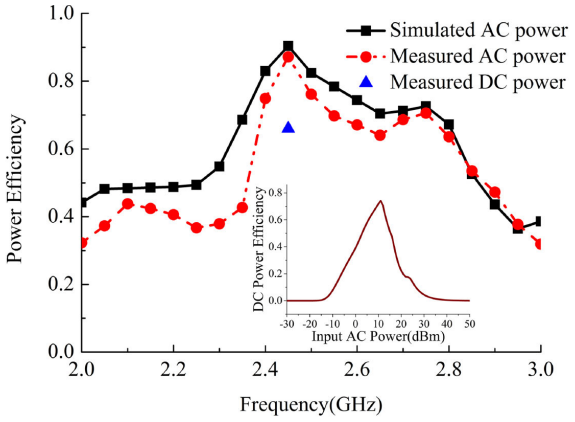

FIGURE 49. Simulated and measured power efficiency of harvester [106].

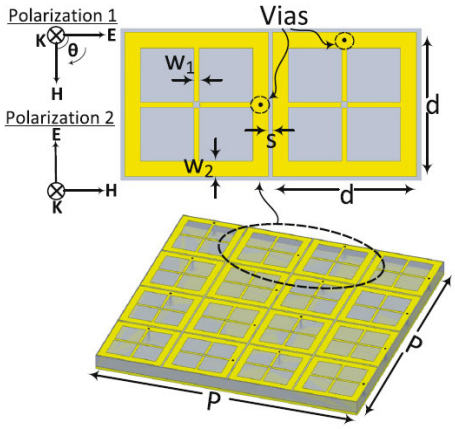

(a)

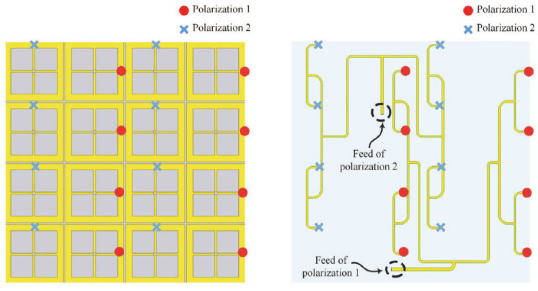

(b)

FIGURE 50. Schematic of dual polarized energy harvester. (a) Super cell of harvester; and (b) back view and front view of feed network [107].

propagation of the AC signal on the corporate feed network due to the uniform phase of ERR metasurface unit cells.

An 8 × 8 ensemble unit cell based metasurface with overall dimensions of 60 mm × 60 mm was designed at 2.72 GHz in [105]. The goal of this work is to maximize the power conversion efficiency between the incident EM radiation and the DC power at the receiving load by channeling all the power of incident waves from all the harvester elements to a single load using a corporate feed network. Fig. 45(a) demonstrates the geometry of the ELC unit cell, and Fig. 45(b) displays the illustration of a metasurface harvester structure.

The conversion efficiency of the simulation was 99.4%, which is an almost 10% increase in efficiency compared to structure proposed in [104], as shown in Fig. 46. The radiation to DC power efficiency of 51% was achieved at resonance frequency of 2.72 GHz (Fig. 47), which is higher compared to the structure demonstrated in [104].

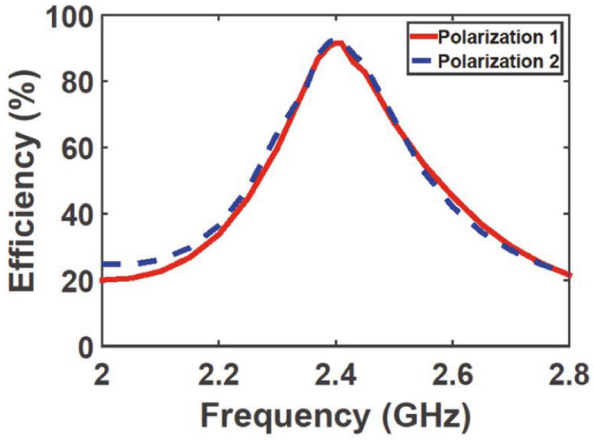

FIGURE 51. Harvester efficiency with feeding network [107].

An EH system based on metamaterial SRR was designed in [106] at 2.45 GHz. The proposed harvester consists of 8×8 resonators to function as a microwave receiving adapter.

Each resonator gathers the power from the ambient environment and delivers all the collected power from all resonators into one output terminal port using an RF combining network. Then, the total delivered AC power is converted into DC current using a single RF rectifying circuit to power a LED load, as illustrated in Fig. 48. As shown in Fig. 49, the measured AC power harvesting efficiency is 86%, the simulated AC power harvesting efficiency is 91%, and the measured AC-to-DC power efficiency is 67%, all at the resonant frequency of 2.45 GHz.

A dual-polarized metasurface harvester for an EM EH system was built in [107] at 2.4 GHz for gathering the power from various incident angles. The harvester consists of 4×4 super cells with alternating vias between neighboring cells that are connected by a feed network as shown in Fig. 50(a). To reduce the feeding ports, cell grouping cells within a super cell is used. The cells are connected by a feed network as shown in Fig. 50(b). The feed network is combined with the super cell metamaterial using an additional layer in the bottom to form three individual layers with two various substrate materials.

The simulated conversion power efficiency of metasurface super cells without rectifier is 92%, as shown in Fig. 51.

Table 3 summarizes in detail several configurations of planar metamaterial/metasurface structures that are used in rectennas for RF EH applications, with concluding remarks.

V. CONCLUSION

Due to advances in lower power wireless devices, the idea of carrying electronics such as wearable or portable devices with self-power could be far closer than the current realization. This paper has reviewed a comprehensive survey on EH and recent advances in metamaterial/metasurface structure based RF EH systems. An overview of EH sources with a focus on RF energy has listed and presented the various kinds of rectenna designs at different operating frequencies. These designs are estimated depending on the power conversion efficiency and antenna size. From reviewed work, it can be very well reasoned that metasurface collectors are better than conventional antennas/arrays. The metasurface antenna with small size and high-power efficiency is very well suited for microwave sensors/rectennas, as it can accomplish high power conversion efficiency with less occupied antenna space. Some techniques, such as a metasurface-based rectenna array connected to one load by a corporate feed network, are suggested to develop good overall rectenna performance, increase the RF-AC/DC power conversion efficiency and reduce the size. Therefore, it can be used in wireless network sensors (WSNs), Internet of Things (IoT), low power sensors/devices and RFID applications.

REFERENCES

[1] C. L. Holloway, E. F. Kuester, J. Baker-Jarvis, and P. Kabos, "A double negative (DNG) composite medium composed of magnetodielectric spherical particles embedded in a matrix," *IEEE Trans. Antennas Propag.*, vol. 51, no. 10, pp. 2596–2603, Oct. 2003.

[2] G. V. Eleftheriades and K. G. Balmain, *Negative-Refraction Metamaterials: Fundamental Principles and Applications*, 1st ed. Hoboken, NJ, USA: Wiley, 2005. [Online]. Available: https://www.wiley.com/en-my/Negative+Refraction+Metamaterials%3A+Fundamental+Principles+and+Applications-p-9780471744740

[3] E. Shamonina and L. Solymar, "Metamaterials: How the subject started," *Metamaterials*, vol. 1, no. 1, pp. 12–18, Mar. 2007.

[4] N. Engheta and R. Ziolkowski, *Metamaterials: Physics and Engineering Explorations*, 1st ed. Hoboken, NJ, USA: Wiley, 2006. [Online]. Available: https://www.wiley.com/en-my/Metamaterials%3A+Physics+and+Engineering+Explorations+-p-9780471784180

[5] J. A. Paradiso and T. Starner, "Energy scavenging for mobile and wireless electronics," *IEEE Pervas. Comput.*, vol. 4, no. 1, pp. 18–27, Jan. 2005.

[6] A. Nechibvute, A. Chawanda, N. Taruvinga, and P. Luhanga, "Radio frequency energy harvesting sources," *Acta Electrotechnica et Inf.*, vol. 17, no. 4, pp. 19–27, Dec. 2017.

[7] M. Pinuela, P. D. Mitcheson, and S. Lucyszyn, "Ambient RF energy harvesting in urban and semi-urban environments," *IEEE Trans. Microw. Theory Techn.*, vol. 61, no. 7, pp. 2715–2726, Jul. 2013.

[8] N. Md. Din, C. K. Chakrabarty, A. Bin Ismail, K. K. A. Devi, and W.-Y. Chen, "Design of RF energy harvesting system for energizing low power devices," *Prog. Electromagn. Res.*, vol. 132, pp. 49–69, 2012.

[9] U. Olgun, J. L. Volakis, and C.-C. Chen, "Design of an efficient ambient WiFi energy harvesting system," *IET Microw., Antennas Propag.*, vol. 6, no. 11, pp. 1200–1206, Aug. 2012.

[10] V. Talla, S. Pellerano, H. Xu, A. Ravi, and Y. Palaskas, "Wi-Fi RF energy harvesting for battery-free wearable radio platforms," in *Proc. IEEE Int. Conf. RFID (RFID)*, Apr. 2015, pp. 47–54.

[11] V. Talla, B. Kellogg, B. Ransford, S. Naderiparizi, S. Gollakota, and J. R. Smith, "Powering the next billion devices with Wi-Fi," in *Proc. 11th ACM Conf. Emerg. Netw. Exp. Technol. CoNEXT*, vol. 60, no. 3, Dec. 2015, pp. 1–13.

[12] Z. Chen, B. Guo, Y. Yang, and C. Cheng, "Metamaterials-based enhanced energy harvesting: A review," *Phys. B, Condens. Matter*, vol. 438, pp. 1–8, Apr. 2014.

[13] S. Kim, R. Vyas, J. Bito, K. Niotaki, A. Collado, A. Georgiadis, and M. M. Tentzeris, "Ambient RF energy-harvesting technologies for self-sustainable standalone wireless sensor platforms," *Proc. IEEE*, vol. 102, no. 11, pp. 1649–1666, Nov. 2014.

[14] S. Roundy, P. K. Wright, and K. S. J. Pister, "Micro-electrostatic vibration-to-electricity converters," in *Proc. Int. Mech. Eng. Congr. Expo. Amer. Soc. Mech. Eng. Digit. Collection ASME*, 2002, pp. 487–496.

[15] S. Cao and J. Li, "A survey on ambient energy sources and harvesting methods for structural health monitoring applications," *Adv. Mech. Eng.*, vol. 9, no. 4, Apr. 2017, Art. no. 168781401769621.

[16] Y. K. Tan and S. K. Panda, "Review of energy harvesting technologies for sustainable wireless sensor network," in *Sustainable Wireless Sensor Networks*. Rijeka, Croatia: IntechOpen, 2010, pp. 15–43. [Online]. Available: https://www.intechopen.com/books/sustainable-wireless-sensor-networks/review-of-energy-harvesting-technologies-for-sustainable-wsn

[17] A. K. Batra and A. Alomari, "Ambient energy sources: Mechanical, light, and thermal," in *Power Harvesting via Smart Materials*. Bellingham, WA, USA: SPIE Press, 2017.

[18] X. Lu, P. Wang, D. Niyato, D. I. Kim, and Z. Han, "Wireless networks with RF energy harvesting: A contemporary survey," *IEEE Commun. Surveys Tuts.*, vol. 17, no. 2, pp. 757–789, 2nd Quart., 2015.

[19] C. A. Balanis, *Antenna Theory: Analysis and Design*. Hoboken, NJ, USA: Wiley, 2016.

[20] X.-X. Yang, C. Jiang, A. Z. Elsherbeni, F. Yang, and Y.-Q. Wang, "A novel compact printed rectenna for data communication systems," *IEEE Trans. Antennas Propag.*, vol. 61, no. 5, pp. 2532–2539, May 2013.

[21] Z. Harouni, L. Cirio, L. Osman, A. Gharsallah, and O. Picon, "A dual circularly polarized 2.45-GHz rectenna for wireless power transmission," *IEEE Antennas Wireless Propag. Lett.*, vol. 10, pp. 306–309, 2011.

[22] Z. Zakaria, N. A. Zainuddin, M. Z. A. Abd Aziz, M. N. Husain, and M. A. Mutalib, "Dual-band monopole antenna for energy harvesting system," in *Proc. IEEE Symp. Wireless Technol. Appl. (ISWTA)*, Sep. 2013, pp. 225–229.

[23] J. H. Kim, S. I. Cho, H.-J. Kim, J.-W. Choi, J. E. Jang, and J. P. Choi, "Exploiting the mutual coupling effect on dipole antennas for RF energy harvesting," *IEEE Antennas Wireless Propag. Lett.*, vol. 15, pp. 1301–1304, 2016.

[24] J. Heikkinen and M. Kivikoski, "A novel dual-frequency circularly polarized rectenna," *IEEE Antennas Wireless Propag. Lett.*, vol. 2, pp. 330–333, 2003.

[25] Y.-J. Ren, M. F. Farooqui, and K. Chang, "A compact dual-frequency rectifying antenna with high-orders harmonic-rejection," *IEEE Trans. Antennas Propag.*, vol. 55, no. 7, pp. 2110–2113, Jul. 2007.

[26] M.-J. Nie, X.-X. Yang, G.-N. Tan, and B. Han, "A compact 2.45-GHz broadband rectenna using grounded coplanar waveguide," *IEEE Antennas Wireless Propag. Lett.*, vol. 14, pp. 986–989, Dec. 2015.

[27] H. Sun and W. Geyi, "A new rectenna using beamwidth-enhanced antenna array for RF power harvesting applications," *IEEE Antennas Wireless Propag. Lett.*, vol. 16, pp. 1451–1454, 2017.

[28] A. Khemar, A. Kacha, H. Takhedmit, and G. Abib, "Design and experiments of a dual-band rectenna for ambient RF energy harvesting in urban environments," *IET Microw., Antennas Propag.*, vol. 12, no. 1, pp. 49–55, Jan. 2018.

[29] A. Mavaddat, S. H. M. Armaki, and A. R. Erfanian, "Millimeter-Wave Energy Harvesting Using 4 X 4 Microstrip Patch Antenna Array," *IEEE Antennas Wireless Propag. Lett.*, vol. 14, no. c, pp. 515–518, 2015.

[30] A. Bakkali, J. Pelegri-Sebastia, T. Sogorb, V. Llario, and A. Bou-Escriva, "A dual-band antenna for RF energy harvesting systems in wireless sensor networks," *J. Sensors*, vol. 2016, pp. 1–8, Jan. 2016.

[31] D. Fang, *Antenna Theory and Microstrip Antennas*, 1st ed. Boca Raton, FL, USA: CRC Press, 2009. [Online]. Available: https://www.routledge.com/Antenna-Theory-and-Microstrip-Antennas/Fang/p/book/9781439807279

[32] S. Agrawal, S. Pandey, J. Singh, and P. N. Kondekar, "An efficient RF energy harvester with tuned matching circuit," in *Communications in Computer and Information Science*, vol. 382. Springer, 2013, pp. 138–145. [Online]. Available: https://link.springer.com/chapter/10.1007/978-3-642-42024-5_17

[33] M. T. Penella-López and M. Gasulla-Forner, *Powering Autonomous Sensors*. Dordrecht, The Netherlands: Springer, 2011.

[34] J. A. Hagerty, F. B. Helmbrecht, W. H. McCalpin, R. Zane, and Z. B. PopovicArt. no. , "Recycling ambient microwave energy with broad-band rectenna arrays," *IEEE Trans. Microw. Theory Techn.*, vol. 52, no. 3, pp. 1014–1024, Mar. 2004.

[35] M. Ghovanloo and K. Najafi, "Fully integrated wideband high-current rectifiers for inductively powered devices," *IEEE J. Solid-State Circuits*, vol. 39, no. 11, pp. 1976–1984, Nov. 2004.

[36] J. P. Curty, M. Declercq, C. Dehollain, and N. Joehl, *Design and Optimization of Passive UHF RFID Systems*. Boston, MA, USA: Springer, 2007.

[37] A. Sihvola, "Metamaterials in electromagnetics," *Metamaterials*, vol. 1, no. 1, pp. 2–11, Mar. 2007.

[38] R. A. Shelby, "Experimental verification of a negative index of refraction," *Science*, vol. 292, no. 5514, pp. 77–79, Apr. 2001.

[39] W.-C. Chen, A. Totachawattana, K. Fan, J. L. Ponsetto, A. C. Strikwerda, X. Zhang, R. D. Averitt, and W. J. Padilla, "Single-layer terahertz metamaterials with bulk optical constants," *Phys. Rev. B, Condens. Matter*, vol. 85, no. 3, Jan. 2012, Art. no. 035112.

[40] D. R. Smith, W. J. Padilla, D. C. Vier, S. C. Nemat-Nasser, and S. Schultz, "Composite medium with simultaneously negative permeability and permittivity," *Phys. Rev. Lett.*, vol. 84, no. 18, pp. 4184–4187, May 2000.

[41] M. Choi, S. H. Lee, Y. Kim, S. B. Kang, J. Shin, M. H. Kwak, K.-Y. Kang, Y.-H. Lee, N. Park, and B. Min, "A terahertz metamaterial with unnaturally high refractive index," *Nature*, vol. 470, no. 7334, pp. 369–373, Feb. 2011.

[42] S. Iyer, S. Popov, and A. T. Friberg, "Effective tunability and realistic estimates of group index in plasmonic metamaterials exhibiting electromagnetically induced transparency," *Appl. Opt.*, vol. 50, no. 21, p. 3958, Jul. 2011.

[43] H. O. Moser and C. Rockstuhl, "3D THz metamaterials from micro/nanomanufacturing," *Laser Photon. Rev.*, vol. 6, no. 2, pp. 219–244, Apr. 2012.

[44] I. Bergmair, B. Dastmalchi, M. Bergmair, A. Saeed, W. Hilber, G. Hesser, C. Helgert, E. Pshenay-Severin, T. Pertsch, E. B. Kley, U. Hübner, N. H. Shen, R. Penciu, M. Kafesaki, C. M. Soukoulis, K. Hingerl, M. Muehlberger, and R. Schoeftner, "Single and multilayer metamaterials fabricated by nanoimprint lithography," *Nanotechnology*, vol. 22, no. 32, Aug. 2011, Art. no. 325301.

[45] Z. H. Jiang, S. Yun, F. Toor, D. H. Werner, and T. S. Mayer, "Conformal dual-band near-perfectly absorbing mid-infrared metamaterial coating," *ACS Nano*, vol. 5, no. 6, pp. 4641–4647, Jun. 2011.

[46] D. Y. Shchegolkov, A. K. Azad, J. F. O'Hara, and E. I. Simakov, "Perfect subwavelength fishnetlike metamaterial-based film terahertz absorbers," *Phys. Rev. B, Condens. Matter*, vol. 82, no. 20, Nov. 2010, Art. no. 205117.

[47] Q. Wen, "Perfect metamaterial absorbers in microwave and Terahertz bands," in *Metamaterial*. Rijeka, Croatia: IntechOpen, 2012, pp. 501–512. [Online]. Available: https://www.intechopen.com/books/metamaterial/perfect-metamaterial-absorbers-in-microwave-and-terahertz-bands

[48] M. Bağmancı, O. Akgöl, M. Özaktürk, M. Karaaslan, E. Ünal, and M. Bakır, "Polarization independent broadband metamaterial absorber for microwave applications," *Int. J. RF Microw. Comput.-Aided Eng.*, vol. 29, no. 1, Jan. 2019, Art. no. e21630.

[49] M. Agarwal, A. K. Behera, and M. K. Meshram, "Wide-angle quad-band polarisation-insensitive metamaterial absorber," *Electron. Lett.*, vol. 52, no. 5, pp. 340–342, Mar. 2016.

[50] J. Hao, J. Wang, X. Liu, W. J. Padilla, L. Zhou, and M. Qiu, "High performance optical absorber based on a plasmonic metamaterial," *Appl. Phys. Lett.*, vol. 96, no. 25, Jun. 2010, Art. no. 251104.

[51] S. Ramya and I. S. Rao, "A compact ultra-thin ultra-wideband microwave metamaterial absorber," *Microw. Opt. Technol. Lett.*, vol. 59, no. 8, pp. 1837–1845, Aug. 2017.

[52] M. R. AlShareef and O. Ramahi, "Energy Harvesting in the Microwaves Spectrum Using Electrically Small Resonators," in *International Congress on Energy Efficiency and Energy Related Materials (ENEFM)*, vol. 155, A. Y. Oral, Z. B. Bahsi, and M. Ozer, Eds. Cham, Switzerland: Springer, 2014, pp. 265–272.

[53] T. Almoneef and O. M. Ramahi, "A 3-dimensional stacked metamaterial arrays for electromagnetic energy harvesting," *Prog. Electromagn. Res.*, vol. 146, pp. 109–115, 2014.

[54] K. S. L. Al-badri, "Electromagnetic broad band absorber based on metamaterial and lumped resistance," *J. King Saud Univ. Sci.*, vol. 32, no. 1, pp. 501–506, Jan. 2020.

[55] E. Karakaya, F. Bagci, S. Can, A. E. Yilmaz, and B. Akaoglu, "Four-band electromagnetic energy harvesting with a dual-layer metamaterial structure," *Int. J. RF Microw. Comput.-Aided Eng.*, vol. 29, no. 1, Jan. 2019, Art. no. e21644.

[56] E. Karakaya, F. Bagci, A. E. Yilmaz, and B. Akaoglu, "Metamaterial-based four-band electromagnetic energy harvesting at commonly used GSM and Wi-Fi frequencies," *J. Electron. Mater.*, vol. 48, no. 4, pp. 2307–2316, Apr. 2019.

[57] S. Khan and T. F. Eibert, "A multi-resonant meta-absorber as an electromagnetic energy harvester," in *Proc. IEEE Int. Symp. Antennas Propag. USNC/URSI Nat. Radio Sci. Meeting*, Jul. 2017, pp. 1091–1092.

[58] G. Fu and S. Sonkusale, "Broadband wireless radio frequency power telemetry using a metamaterial resonator embedded with non-foster impedance circuitry," *Appl. Phys. Lett.*, vol. 106, no. 20, May 2015, Art. no. 203504.

[59] C. Mulazimoglu, E. Karakaya, S. Can, A. E. Yilmaz, and B. Akaoglu, "Hexagonal-shaped metamaterial energy harvester design," in *Proc. 10th Int. Congr. Adv. Electromagn. Mater. Microw. Opt. (METAMATERIALS)*, Sep. 2016, pp. 82–84.

[60] A. M. Hawkes, A. R. Katko, and S. A. Cummer, "A microwave metamaterial with integrated power harvesting functionality," *Appl. Phys. Lett.*, vol. 103, no. 16, Oct. 2013, Art. no. 163901.

[61] X. Duan, X. Chen, and L. Zhou, "A metamaterial electromagnetic energy rectifying surface with high harvesting efficiency," *AIP Adv.*, vol. 6, no. 12, Dec. 2016, Art. no. 125020.

[62] S. Shang, S. Yang, J. Liu, M. Shan, and H. Cao, "Metamaterial electromagnetic energy harvester with high selective harvesting for left- and right-handed circularly polarized waves," *J. Appl. Phys.*, vol. 120, no. 4, Jul. 2016, Art. no. 045106.

[63] M. Karaaslan, M. Bağmancı, E. Ünal, O. Akgol, O. Altıntaş, and C. Sabah, "Broad band metamaterial absorber based on wheel resonators with lumped elements for microwave energy harvesting," *Opt. Quantum Electron.*, vol. 50, no. 5, p. 225, May 2018.

[64] F. O. Alkurt, O. Altintas, M. Bakir, A. Tamer, F. Karadag, M. Bagmanci, M. Karaaslan, E. Unal, and O. Akgol, "Octagonal shaped metamaterial absorber based energy harvester," *Mater. Sci.*, vol. 24, no. 3, pp. 253–259, 2018.

[65] C. M. Soukoulis and M. Wegener, "Past achievements and future challenges in the development of three-dimensional photonic metamaterials," *Nature Photon.*, vol. 5, no. 9, pp. 523–530, Sep. 2011.

[66] H.-T. Chen, A. J. Taylor, and N. Yu, "A review of metasurfaces: Physics and applications," *Rep. Prog. Phys.*, vol. 79, no. 7, Jul. 2016, Art. no. 076401.

[67] N. Yu and F. Capasso, "Flat optics with designer metasurfaces," *Nature Mater.*, vol. 13, no. 2, pp. 139–150, Feb. 2014.

[68] C. L. Holloway, A. Dienstfrey, E. F. Kuester, J. F. O'Hara, A. K. Azad, and A. J. Taylor, "A discussion on the interpretation and characterization of metafilms/metasurfaces: The two-dimensional equivalent of metamaterials," *Metamaterials*, vol. 3, no. 2, pp. 100–112, Oct. 2009.

[69] C. L. Holloway, E. F. Kuester, J. A. Gordon, J. O'Hara, J. Booth, and D. R. Smith, "An overview of the theory and applications of metasurfaces: The two-dimensional equivalents of metamaterials," *IEEE Antennas Propag. Mag.*, vol. 54, no. 2, pp. 10–35, Apr. 2012.

[70] J. Wang and J. Du, "Plasmonic and dielectric metasurfaces: Design, fabrication and applications," *Appl. Sci.*, vol. 6, no. 9, p. 239, 2016.

[71] N. Yu, P. Genevet, F. Aieta, M. A. Kats, R. Blanchard, G. Aoust, J.-P. Tetienne, Z. Gaburro, and F. Capasso, "Flat optics: Controlling wavefronts with optical antenna metasurfaces," *IEEE J. Sel. Topics Quantum Electron.*, vol. 19, no. 3, May 2013, Art. no. 4700423.

[72] M. A. Kats, R. Blanchard, P. Genevet, and F. Capasso, "Nanometre optical coatings based on strong interference effects in highly absorbing media," *Nature Mater.*, vol. 12, no. 1, pp. 20–24, Jan. 2013.

[73] X. Luo, "Principles of electromagnetic waves in metasurfaces," *Sci. China Phys., Mech. Astron.*, vol. 58, no. 9, Sep. 2015, Art. no. 594201.

[74] L. B. Wang, K. Y. See, J. W. Zhang, B. Salam, and A. C. W. Lu, "Ultra-thin and flexible screen-printed metasurfaces for EMI shielding applications," *IEEE Trans. Electromagn. Compat.*, vol. 53, no. 3, pp. 700–705, Aug. 2011.

[75] M. M. Masud, B. Ijaz, A. Iftikhar, M. N. Rafiq, and B. D. Braaten, "A reconfigurable dual-band metasurface for EMI shielding of specific electromagnetic wave components," in *Proc. IEEE Int. Symp. Electromagn. Compat.*, Aug. 2013, pp. 640–644.

[76] M. M. Masud, B. Ijaz, I. Ullah, and B. Braaten, "A compact dual-band EMI metasurface shield with an actively tunable polarized lower band," *IEEE Trans. Electromagn. Compat.*, vol. 54, no. 5, pp. 1182–1185, Oct. 2012.

[77] H. Zhong and X. Yang, "Broadband meta-surface with polarization-insensitive and wide-angle for electromagnetic energy harvesting," in *Proc. Int. Workshop Antenna Technology: Small Antennas, Innov. Struct., Appl. (iWAT)*, 2017, pp. 125–128.

[78] M. E. Badawe and O. M. Ramahi, "Metasurface for near-unity electromagnetic energy harvesting and wireless power transfer," in *Proc. IEEE Int. Symp. Antennas Propag. (APSURSI)*, Jun. 2016, pp. 609–610.

[79] X. Duan, X. Chen, and L. Zhou, "A metamaterial harvester with integrated rectifying functionality," in *Proc. IEEE/ACES Int. Conf. Wireless Inf. Technol. Syst. (ICWITS) Appl. Comput. Electromagn. (ACES)*, Mar. 2016, pp. 1–2.

[80] B. M. Z. 'Abidin, O. O. Khalifa, E. M. A. Elsheikh, and A. H. Abdulla, "Wireless energy harvesting for portable devices using split ring resonator," in *Proc. Int. Conf. Comput., Control, Netw., Electron. Embedded Syst. Eng. (ICCNEEE)*, Sep. 2015, pp. 362–367.

[81] W. Hu, Z. Yang, F. Zhao, G. Wen, J. Li, Y. Huang, D. Inserra, and Z. Chen, "Low-cost air gap metasurface structure for high absorption efficiency energy harvesting," *Int. J. Antennas Propag.*, vol. 2019, pp. 1–8, Sep. 2019.

[82] X. Zhang and L. Li, "A dual-band polarization-independent and wide-angle metasurface for electromagnetic power harvesting," in *Proc. 6th Asia–Pacific Conf. Antennas Propag. (APCAP)*, Oct. 2017, pp. 1–3.

[83] W. Hu, D. Inserra, Y. Huang, J. Li, G. Wen, J. Xie, and W. Zhu, "High efficiency electromagnetic energy harvesting with metasurface," in *Proc. IEEE Asia–Pacific Conf. Antennas Propag. (APCAP)*, Aug. 2018, pp. 488–489.

[84] S. F. Babazadeh, M. Khanjarian, M. El Badawe, V. Nayyeri, M. Soleimani, and O. M. Ramahi, "A circularly polarized metasurface antenna," in *Proc. 12th Eur. Conf. Antennas Propag. (EuCAP)*, 2018, p. 333.

[85] W. E. I. Liu, Z. N. Chen, X. Qing, J. Shi, and F. H. Lin, "Miniaturized wideband metasurface antennas," *IEEE Trans. Antennas Propag.*, vol. 65, no. 12, pp. 7345–7349, Dec. 2017.

[86] S. U. Rahman, Q. Cao, I. Gil, M. Sajjad, and Y. Wang, "Design of wideband beamforming metasurface with alternate absorption," *IEEE Access*, vol. 8, pp. 21393–21400, 2020.

[87] O. M. Ramahi, T. S. Almoneef, M. AlShareef, and M. S. Boybay, "Metamaterial particles for electromagnetic energy harvesting," *Appl. Phys. Lett.*, vol. 101, no. 17, Oct. 2012, Art. no. 173903.

[88] B. Alavikia, T. S. Almoneef, and O. M. Ramahi, "Complementary split ring resonator arrays for electromagnetic energy harvesting," *Appl. Phys. Lett.*, vol. 107, no. 3, Jul. 2015, Art. no. 033902.

[89] Q. Zhao, L. Li, X. Zhang, X. Zhang, and J. Chen, "An ambient energy harvester using metasurface," in *Proc. IEEE Int. Symp. Electromagn. Compat. IEEE Asia–Pacific Symp. Electromagn. Compat. (EMC/APEMC)*, May 2018, pp. 111–112.

[90] B. Alavikia, T. S. Almoneef, and O. M. Ramahi, "Wideband resonator arrays for electromagnetic energy harvesting and wireless power transfer," *Appl. Phys. Lett.*, vol. 107, no. 24, Dec. 2015, Art. no. 243902.

[91] X. Zhang, H. Liu, and L. Li, "Electromagnetic power harvester using wide-angle and polarization-insensitive metasurfaces," *Appl. Sci.*, vol. 8, no. 4, p. 497, 2018.

[92] T. S. Almoneef and O. M. Ramahi, "Metamaterial electromagnetic energy harvester with near unity efficiency," *Appl. Phys. Lett.*, vol. 106, no. 15, Apr. 2015, Art. no. 153902.

[93] B. Ghaderi, V. Nayyeri, M. Soleimani, and O. M. Ramahi, "A novel symmetric ELC resonator for polarization-independent and highly efficient electromagnetic energy harvesting," in *IEEE MTT-S Int. Microw. Symp. Dig.*, Sep. 2017, pp. 1–3.

[94] A. Ghaneizadeh, K. Mafinezhad, and M. Joodaki, "Design and fabrication of a 2D-isotropic flexible ultra-thin metasurface for ambient electromagnetic energy harvesting," *AIP Adv.*, vol. 9, no. 2, Feb. 2019, Art. no. 025304.

[95] X. Duan, X. Chen, Y. Zhou, L. Zhou, and S. Hao, "Wideband metamaterial electromagnetic energy harvester with high capture efficiency and wide incident angle," *IEEE Antennas Wireless Propag. Lett.*, vol. 17, no. 9, pp. 1617–1621, Sep. 2018.

[96] F. Yu, X. Yang, H. Zhong, C. Chu, and S. Gao, "Polarization-insensitive wide-angle-reception metasurface with simplified structure for harvesting electromagnetic energy," *Appl. Phys. Lett.*, vol. 113, no. 12, Sep. 2018, Art. no. 123903.

[97] B. Ghaderi, V. Nayyeri, M. Soleimani, and O. M. Ramahi, "Pixelated metasurface for dual-band and multi-polarization electromagnetic energy harvesting," *Sci. Rep.*, vol. 8, no. 1, p. 13227, Dec. 2018.

[98] X. Zhang, H. Liu, and L. Li, "Tri-band miniaturized wide-angle and polarization-insensitive metasurface for ambient energy harvesting," *Appl. Phys. Lett.*, vol. 111, no. 7, Aug. 2017, Art. no. 071902.

[99] H.-T. Zhong, X.-X. Yang, X.-T. Song, Z.-Y. Guo, and F. Yu, "Wide-band metamaterial array with polarization-independent and wide incident angle for harvesting ambient electromagnetic energy and wireless power transfer," *Appl. Phys. Lett.*, vol. 111, no. 21, Nov. 2017, Art. no. 213902.
[100] S. D. Assimonis, T. Kollatou, D. Tsiamitros, D. Stimoniaris, T. Samaras, and J. N. Sahalos, "High efficiency and triple-band metamaterial electromagnetic energy hervester," in *Proc. 9th Int. Conf. Electr. Electron. Eng. (ELECO)*, Nov. 2015, pp. 320–323.
[101] H.-T. Zhong, X.-X. Yang, C. Tan, and K. Yu, "Triple-band polarization-insensitive and wide-angle metamaterial array for electromagnetic energy harvesting," *Appl. Phys. Lett.*, vol. 109, no. 25, Dec. 2016, Art. no. 253904.
[102] B. Ghaderi, V. Nayyeri, M. Soleimani, and O. M. Ramahi, "Multi-polarisation electromagnetic energy harvesting with high efficiency," *IET Microw., Antennas Propag.*, vol. 12, no. 15, pp. 2271–2275, Dec. 2018.
[103] G. T. Oumbé Tékam, V. Ginis, J. Danckaert, and P. Tassin, "Designing an efficient rectifying cut-wire metasurface for electromagnetic energy harvesting," *Appl. Phys. Lett.*, vol. 110, no. 8, Feb. 2017, Art. no. 083901.
[104] M. El Badawe, T. S. Almoneef, and O. M. Ramahi, "A metasurface for conversion of electromagnetic radiation to DC," *AIP Adv.*, vol. 7, no. 3, Mar. 2017, Art. no. 035112.
[105] M. El Badawe and O. M. Ramahi, "Efficient metasurface rectenna for electromagnetic wireless power transfer and energy harvesting," *Prog. Electromagn. Res.*, vol. 161, pp. 35–40, 2018.
[106] P. Xu, S. Y. Wang, and W. Geyi, "Design of an effective energy receiving adapter for microwave wireless power transmission application," *AIP Adv.*, vol. 6, no. 10, 2016, Art. no. 105010, doi: 10.1063/1.4966050.
[107] T. S. Almoneef, F. Erkmen, and O. M. Ramahi, "Harvesting the energy of multi-polarized electromagnetic waves," *Sci. Rep.*, vol. 7, no. 1, p. 14656, Dec. 2017.

ABDULRAHMAN AHMED GHALEB AMER received the B.Sc. degree from the Department of Electrical and Electronic Engineering, Aleppo University, Syria, in 2012, and the M.Sc. degree from University Tun Hussein Onn Malaysia (UTHM), in 2017, where he is currently pursuing the Ph.D. degree. His research interests include the analysis of metamaterial and metasurface for energy harvesting and antenna applications.

SYARFA ZAHIRAH SAPUAN (Member, IEEE) received the B.Eng. degree (Hons.) in electrical engineering from Kolej Universiti Tun Hussein Onn Malaysia (UTHM), Batu Pahat, Malaysia, in 2003, the M.Sc. degree in communication engineering from Nanyang Technological University, Singapore, in 2009, and the Ph.D. degree in electrical engineering from UTHM, in 2014. She is currently a Senior Lecturer with the Communication Engineering Department, UTHM, where she is also a Principle Researcher of the Electromagnetic Compatibility Research Cluster at the Research Center for Applied Electromagnetics. Her research interests include electromagnetic compatibility, antenna calibration, and RF energy harvesting.

NASIMUDDIN NASIMUDDIN (Senior Member, IEEE) received the B.Sc. degree from JMI, in 1994, and the M.Tech. and Ph.D. degrees from the University of Delhi, India, in 1998 and 2004, respectively. He has worked as a Senior Research Fellow in DST sponsored project and Council of Scientific and Industrial Research (CSIR) grant Senior Research Fellowship in Engineering Science at the Department of Electronic Science, University of Delhi, from 1999 to 2003. He has worked as an Australian Postdoctoral Research Fellow in awarded Discovery project grant from Australian Research Council at the Macquarie University, Australia, from 2004 to 2006. He is currently working as a Scientist with the Institute for Infocomm Research, Singapore. He has published 168 journal and conference technical papers. He has edited and contributed a chapter to a book *Microstrip Antennas* (InTech, 2011). His research interests include multilayered microstrip-based structures, millimeter-wave, RFID reader, GPS/GNSS, satellite, TV white space, RF energy harvesting systems, UWB, beam-scanning/beamforming, metamaterial, and CP microstrip antennas. He is a Senior Member of the IEEE Antennas and Propagation Society. He was awarded a senior research fellowship from the Council of Scientific and Industrial Research, Government of India in Engineering Science, from 2001 to 2003, a Discovery Projects fellowship from the Australian Research Council, from 2004 to 2006, the Singapore Manufacturing Federation Award (with project team), in 2014, and the Young Scientist Award from the International Union of Radio Science (URSI), in 2005.

AROKIASWAMI ALPHONES (Senior Member, IEEE) received the B.Tech. degree from the Madras Institute of Technology, in 1982, the M.Tech. degree from the Indian Institute of Technology Kharagpur, in 1984, and the Ph.D. degree in optically controlled millimeter wave circuits from the Kyoto Institute of Technology, Japan, in 1992. He was a JSPS Visiting Fellow at Japan, from 1996 to 1997. From 1997 to 2001, he was with the Centre for Wireless Communications, National University of Singapore, involved in the research on optically controlled passive/active devices. Since 2001, he has been with the School of Electrical and Electronic Engineering, Nanyang Technological University, Singapore. He has 34 years of research experience. He has published and presented over 300 technical articles in peer reviewed International journals/conferences. His current interests are electromagnetic analysis on planar RF circuits and integrated optics, microwave photonics, metamaterial-based leaky wave antennas, wireless power transfer technologies, and visible light positioning. He was involved with many IEEE flagship conferences held in Singapore and General Chair of APMC 2009, MWP 2011, TENCON 2016, and APMC 2019. He was the Chairman of IEEE Singapore Section, in 2015, 2016, 2018. He was also the Panel member of the IEEE Conference Quality Committee.

NABIAH BINTI ZINAL received the Diploma degree in telecommunication engineering from Universiti Teknologi Malaysia (UTM), Kuala Lumpur, in 1997, the B.Eng. degree (Hons.) in electrical engineering from Universiti Teknologi Malaysia (UTM), Skudai, Malaysia, in 1999, and the M.Sc. degree in telecommunication engineering from Kolej Universiti Teknologi Tun Hussien Onn, Malaysia, in 2004. She is currently a Senior Lecturer with the Center of Diploma Studies, Electrical Engineering Department, UTHM. Her research interests include electromagnetic compatibility, electronics measurement and calibration, and the IoT application.